NTNU – Trondheim
Norwegian University of
Science and Technology

Assessing Weighting Coefficients in Seismic History Matching of the Norne Field

Simen Nygaard

Master of Science in Engineering and ICT
Submission date: June 2013
Supervisor: Jon Kleppe, IPT

Norwegian University of Science and Technology
Department of Petroleum Engineering and Applied Geophysics

"Every home is a university and the parents are the teachers."

— Mahatma Gandhi, The Wit and Wisdom of Gandhi

Summary

4D seismic data has become an important tool for oil and gas field operators. Reservoir characterization, evaluation and monitoring are all improved by including seismic data in the history matching routine.

History matching is a process for improving the model by changing its parameters until it reproduces the observed data.

Regular history matching tries to get the model to reproduce the fluid production in a quite simple mass balance situation. With the integration of seismic data, the actual fluid flow can be reproduced, making the history match better and the reservoir model more reliable.

The Norne field is a Statoil-operated oil and gas field, located in the Norwegian Sea. Available simulation model and other engineering data makes it possible to do a history matching study on the field.

Semi-automatic seismic history matching was performed with SimOpt, and the combination of weighting coefficients was altered to find the best combination.

The auto-balanced case outperformed the other combinations, and decreased the total RMS value 0.5%.

Sammendrag

4D-seismikk er blitt et viktig verktøy for operatører av olje-og gassfelt. Reservoarkarakterisering, -evaluering og -overvåking blir forbedret ved å inkludere seismiske data i historietilpasningsprosessen.

Historietilpasning er en fremgangsmåte for å forbedre reservoarmodellen ved å endre parametrene til den reproduserer de observerte data. Vanlig historietilpasning prøver å få modellen til å reprodusere fluidproduksjonen med en ganske enkel massebalanse. Med integreringen av seismiske data kan den faktiske fluidstrømmen reproduseres, slik at historietilpasningen blir bedre og reservoarmodellen mer pålitelig.

Norne-feltet er et Statoil-operert olje-og gassfelt som ligger i Nordsjøen. Tilgjengeliggjøring av simuleringsmodellen og andre tekniske data som produksjonstall og brønnbaner har gjort det mulig å utføre en historietilpasningsanalyse på feltet.

Semi-automatisk seismisk historietilpasning ble utført med SimOpt, og kombinasjonen av veiekoeffisienter ble endret for å finne den beste kombinasjonen. Den auto-balanserte kombinasjonen leverte de beste resultatene, og redusert den totale RMS-verdien med 0,5%.

Acknowledgments

This master thesis has been supervised by Professor Jon Kleppe, whom I would like to thank for his guidance and well-proven expertise.

I would like to thank my fellow students for providing a good working environment with skilled support and space for both social contact and times of silence and concentration.

Likewise, I would like to thank:

Alexey Stovas, Professor of Geophysics in the Department of Petroleum Engineering and Applied Geophysics at NTNU, for helping me with the seismic data and for answering my questions related to these.

Jan Ivar Jensen, Assistant Professor in the Department of Petroleum Engineering and Applied Geophysics at NTNU, for providing me help with the simulator and other reservoir engineering problems.

Trine Alsos, Statoil, for providing the additional data I needed and for answering my questions about seismic data, history matching and the Norne field.

Lastly, I would like to thank my family, especially my two brothers, for both their ability to torment me and their ability to make me laugh.

Trondheim, June 16, 2013

Simen Nygaard

Table of contents

List of figures

List of tables

1 Introduction

4D seismic data has become an important tool for oil and gas field operators. Reservoir characterization, evaluation and monitoring are all improved by including seismic data in the history matching routine. A lot of business decisions in an oil and gas company, and for other stakeholders, are based on the reservoir model. The predictions for future production and drainage of the reservoir are based heavily on the reservoir model. History matching is a process for improving the model by changing its parameters until it reproduces the observed data. Regular history matching tries to get the model to reproduce the fluid production in a quite simple mass balance situation. With the integration of seismic data, the actual fluid flow can be reproduced, making the history match better and the reservoir model more reliable. (Nygaard, 2012)

Qualitative analysis and inclusion of time-lapse seismic data has been an important and valuable tool – returning the implementation cost – like cost of seismic acquisition and the cost of adapting the personnel and software to a new workflow - back to the oil companies with interest. This development has provided invaluable information, used to locate remaining hydrocarbons in the reservoirs. By analyzing the fluid flow directly, engineers are able to spot possibilities for pockets of undrained hydrocarbons. The uncertainty of the reservoir is diminished, allowing the engineers to make better and more supported decisions for the development of the field. By optimizing the position of infill wells and reducing the uncertainty related to drilling, the number of failed wells, and so the total well cost of the field is minimized.

Quantification of the time-lapse changes is a more frequently used method for increasing hydrocarbon recovery of mature fields. This is now possible due to the increased computing power and development of new techniques and theories. Seismic data integration enhances the ability of the organization to adopt a quantitative approach to the field improvement. The seismic data has to be integrated with well logs, production and injection data and geological knowledge. All available and relevant data should be used to condition the dynamic reservoir model – 4D seismic data should be included in the history

matching process. Overall, time-lapse seismic data increases the understanding of the reservoir.

In this thesis, the Statoil-operated Norne field will be presented together with history matching in general and the integration of seismic data. Semi-automatic history matching with time-lapse seismic will be applied to the Norne field and choice of weighting coefficients will be discussed.

2 Norne

Norne is a Statoil-operated oil and gas field, located in the Norwegian Sea at 380 m sea depth. The field span the two blocks 6508/1 and 6608/10 about 200 km west of the coast of Helgeland and Sandnessjøen, as seen in fFigure 1. This region of the Norwegian Sea is addressed as the southern part of the Nordland II area, and there are several other fields in the near proximity, like Heidrun and Skarv. The field is operated from the offices of Statoil in Harstad.

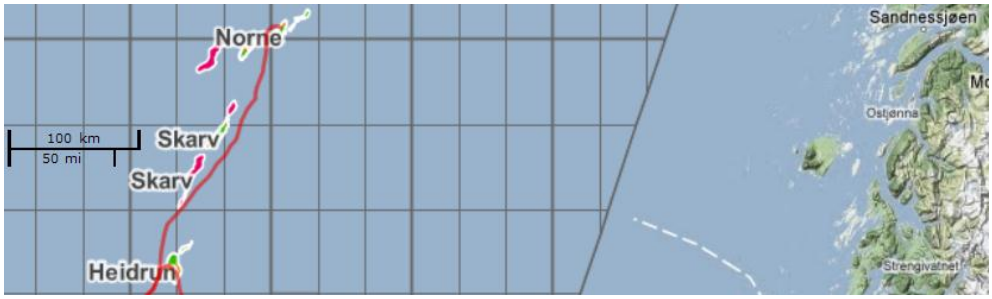

Figure 1: Norne location map (Oljemuseum, 2013b)

Discovery of Norne was done with well 6608/10-2, which found a hydrocarbon column of 135 m consisting of 110 m oil and a gas cap of 25 m in 1991. The field reserves were proven in 1992, and production started November 6th 1997. Norne is co-owned by Statoil as operator with 39.1% ownership, Petoro owning 54% and Eni Norge holding a 6.9% interest in the field, as summarized in tTable 1.

Table 1: Current shareholders of the Norne production licences

Company name	Company share
Petoro AS	54.0 %
Statoil Petroleum AS	39.1 %
Eni Norge	6.9 %

2.1 Reservoir Information

The Norne reservoir was accumulated in a horst block, which covers an area of about 9x3km subsurface. The reservoir is situated at a depth of approximately 2500 m in the Lower to Middle Jurassic sandstones, and is subdivided into four different hydrocarbon bearing formations. From the top, these are Garn, Ile, Tilje and Tofte. In between Garn and Ile lies the stratigraphic layer called Not. The Not formation consists of shale that functions as a seal, so there are no fluid contact between the Garn formation and the underlying Ile-

/Tilje-/Tofte-formations. The field consists of two separate oil compartments, Norne Main Structure and the Northeast Segment (G-segment). The Main Structure contains about 97% of the proven oil. (Statoil, 2004)

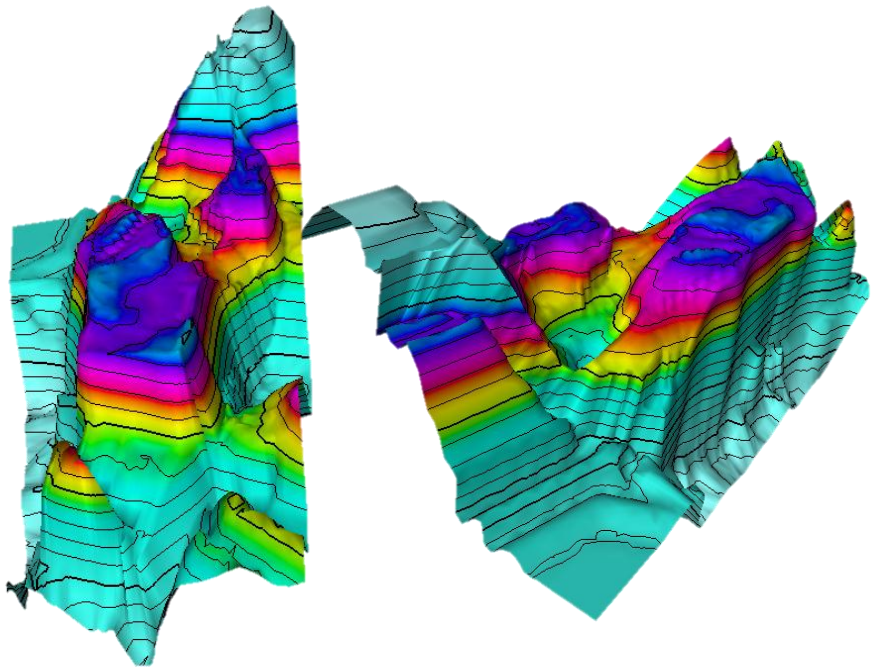

Figure 2: Stratigraphic visualization of the Norne simulator model

The Norne Main Structure can be seen in Figure 2, as the large blue area. It is relative flat with gas in the Garn formation and gas-oil contact close to the Not formation. The Northeast Segment can be seen in the same figure, as the other large blue area. More information of the reservoir, like oil-water contact levels can be seen in (Statoil, 2004). The informative thesis of (Verlo and Hetland, 2008) describes the Norne geology, reservoir properties and fluid properties extensively.

2.2 Development

Norne is produced by a floating production-, storage- and offloading vessel, a FPSO, that rotates around a central turret that is moored to the sea bottom. This construction stabilizes the flexible risers by allowing the ship to rotate to compensate for the shifting waves and weather, while the risers and umbilicals have a stable connection point to the turret. The risers transport the fluids from

the subsea templates and into the processing and storage facility on board the ship, while the umbilicals transmit power to, and data from, the well templates.

The produced oil is offloaded on shuttle tankers, while the produced gas is transported through gas pipes. Norne Gas Export Pipeline and Åsgard Transport trunk line transport the gas 1400 km to Dornum in Germany through the plant at Kårstø. Gas export was initiated in 2001. Both Urd and Alve gas streams have been connected to the Norne facility subsequently, see Figure 3.

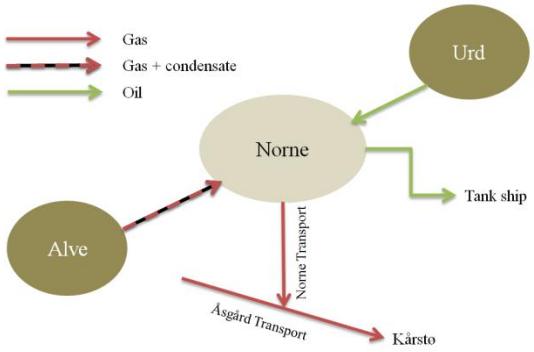

Figure 3: Transport infrastructure in Norne area (Adapted from Oljemuseum (2013a))

Since the first exploration well that found the first hydrocarbons of Norne, an additional 50 wells have been drilled. 33 producing wells have been drilled, but only 16 of them are still active. 8 out of 10 drilled injector wells is still injecting, and a total of 7 observation wells have been completed. From the beginning of production, gas was injected into the gas cap in addition to the water injection in the water zone. After establishing the fact that the Not formation is completely sealing gas injection ceased, and all produced gas was planned exported. To maintain the pressure, gas is now again injected in the reservoir, but mainly in the formations below the seal.

The most recently updated reserves estimations for the Norne field is presented by NPD and represents the situation at the end of 2012, see Table 2. Original oil volume in place, OOIP, for the field is estimated to be 160.8×10^6 Sm^3 and the original gas volume in place is estimated to be 27.06×10^9 Sm3. Recoverable portion of this volume is stipulated to be 90.80×10^6 Sm^3. The Norwegian Petroleum Directorate has estimated the remaining reserves as 3.80 mill Sm^3 oil, 5.40 bill Sm^3 gas and 0.80 mill tonnes of NGL, as of 1.1.2012. (NPD, 2012) This implies that expected ultimate oil recovery is 56.5% of OOIP,

and that 54.1% had already been produced at the end of year 2012. The Norne FPSO has produced 24.3% of the original gas in place, and it is expected that a gas recovery factor of 44.4% is expected before the field is shut down.

Table 2: Reserves estimates by the Norwegian Petroleum Department of 31.12.2012

Orig. recoverable oil [mill Sm3]	Orig. recoverable gas [1000 mill Sm3]	Orig. recoverable NGL [mill tonne]	Orig. recoverable oil equivalents [mill Sm3 o.e.]
90.80	12.00	1.60	105.84
Recoverable oil [mill Sm3]	Recoverable gas [1000 mill Sm3]	Recoverable NGL [mill tonne]	Recoverable oil equivalents [mill Sm3 o.e.]
3.80	5.40	0.80	10.72

2.3 The simulation model

The simulation model of the Norne field is built for the ECLIPSE 100 simulator of Schlumberger. ECLIPSE 100 is fully implicit, three phase and three dimensional black oil simulator from Schlumberger(Schlumberger, 2008b). The model was constructed based on the 2004 geological model.

The model consists of 113344 grid cells, of which 44431 are active, which distributes as 22 layers of 46x112 grid block. The cells are defined in corner point geometry, meaning all cells are unequal and non-regular. This means that each cell has a unique volume and side lengths. DX ranges from 25 to 195 meters, DY ranges from 50 to 270 meters and DZ ranges from 0.2 to 50 meters – but the average grid cell size is about 100m x 100m x 25m.

Porosities, permeabilties and net-to-gross properties are upscaled from the geological model. Vertical permeability was set to a ratio of the horizontal permeability. Oil saturation values can be seen in fFigure 4, and it is possible to identify the gas cap and water aquifer by the areas of pink grid blocks located above and below the oil-saturated zone.

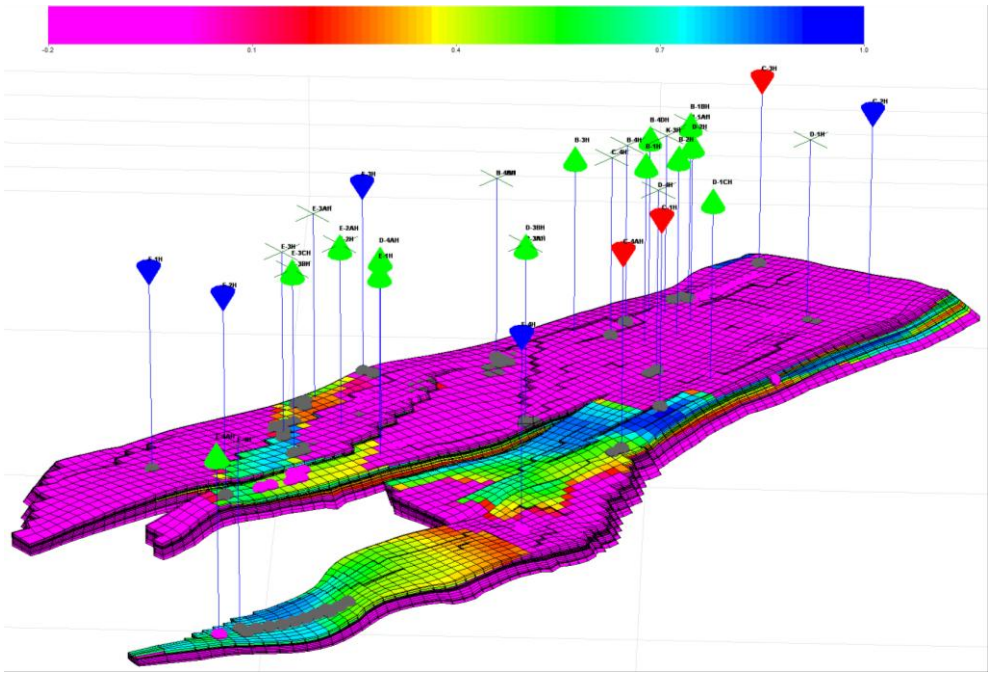

Figure 4: The Norne simulation model visualized with oil saturation values in grid cells. Status and position of well bores shown as they were in late 2006. Blue wells are water injectors, red wells gas injectors and green wells is the fluid producers.Grey cells show well paths.

2.4 Seismic data

The first 3D-survey of the Norne field area was acquired in 1992 in connection to the discovery and the assessment of the hydrocarbon potential of the finding. This was a conventional 3D seismic survey that was used to decide upon developing the field and plan the progress of the development. The first seismic survey that was done with the thought of establishing time-lapse monitoring of the field and its fluid flow was conducted in 2001. This survey was named ST0113, and the resulting survey data is used, and defined, as the base survey of the Norne field. Later, several monitor surveys have been conducted over the Norne area making time-lapse analysis possible. These were conducted in 2003, 2004, 2006 and 2008.

To be able to monitor the fluid flow through the change of acoustic reflectivity with some certainty, monitor surveys have to be similar to the base survey. This ensures that the repeatability of the data is sufficient, and that the monitor survey represents the same geographical and stratigraphic location as the base survey. Q-marine

active streamer steering from WesternGeco was used for all monitor surveys to ensure the necessary repeatability. The Norne FPSO was undershot by a two-vessel operation with one seismic ship firing the air guns from one side, while another seismic ship towed listening cables on the opposite side of the production facility. A repeatability map can be seen in Figure 5.

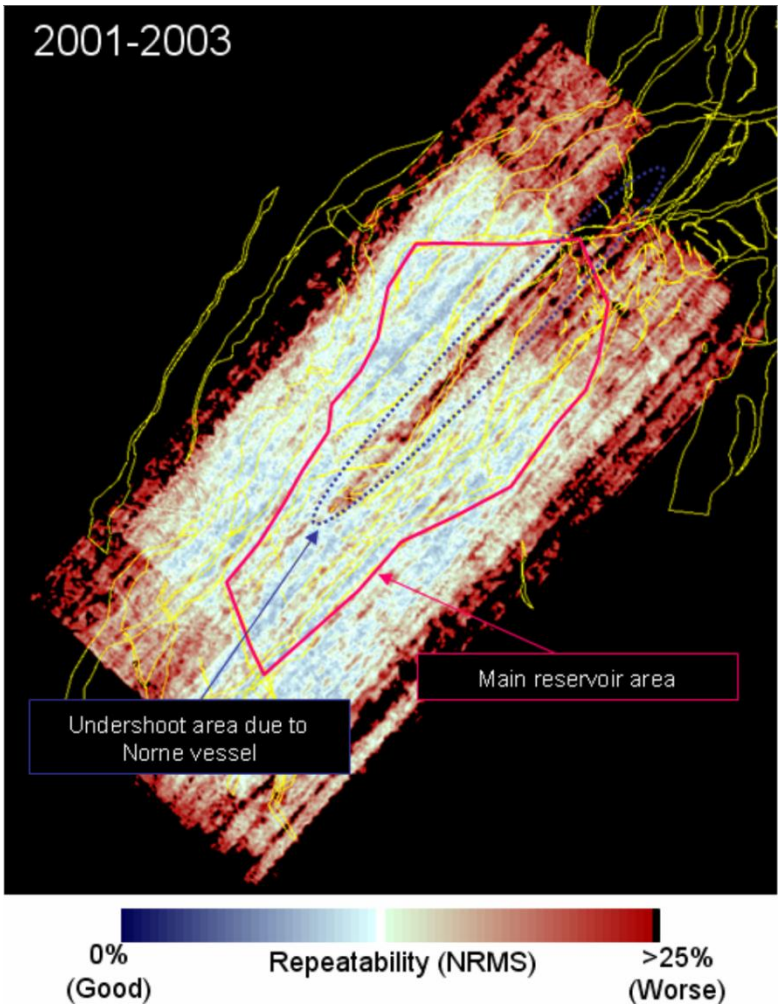

Figure 5: Time-lapse repeatability map of the seismic data for the Norne field. The values are representative for the changes between the base survey and the 2003 monitor survey. Blue and white areas represent areas with good repeatability of the seismic data for that particular area, whereas the red and black areas show the opposite. There is a significant zone with poorer data quality below the Norne vessel. (El Ouair et al., 2005)

Available to scientists, students and other interested parties are several different time-lapse seismic data sets, like difference cubes for the change between the base survey in 2001 and the individual

monitor surveys of 2003, 2004 and 2006. Cubes of calculated pore pressure, gas saturation and water saturation are available, together with far-, mid- and near-stack time-lapsed survey data for base survey and the three earliest monitor surveys. How the seismic data was processed is thoroughly described in (Glenister and Otterbein, 2007). Examples of time-lapse seismic data are presented in Figure 6, Figure 7 and Figure 8.

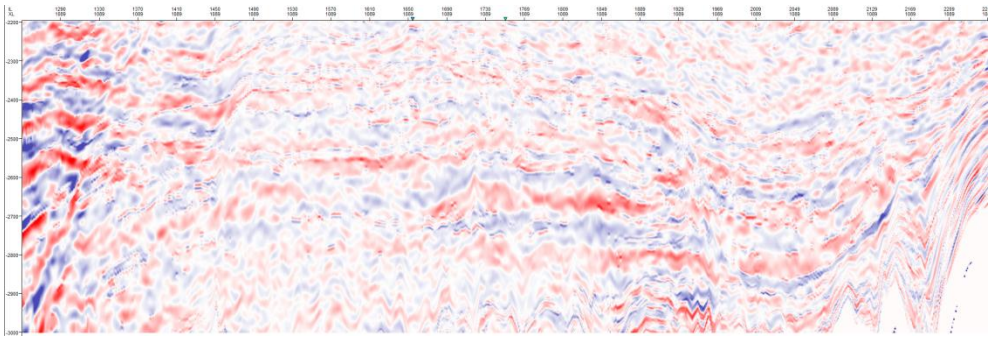

Figure 6: Time-lapse seismic. Relative change in acoustic impedance between 2006 and 2001. Crossline number 1089.

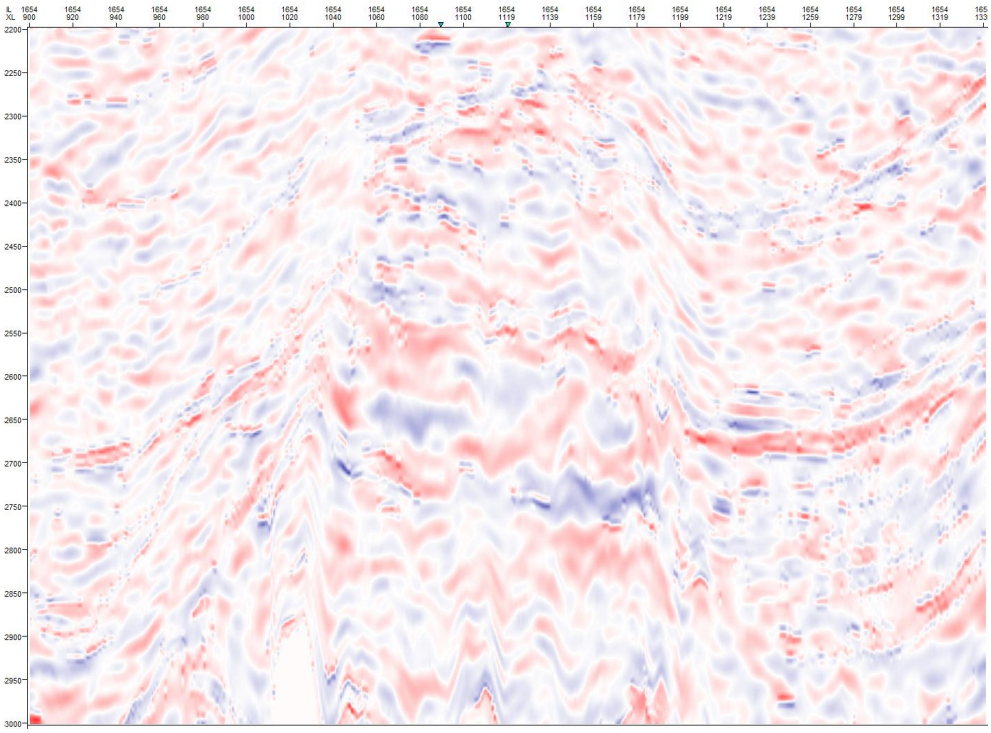

Figure 7: Time-lapse seismic. Relative change in acoustic impedance between 2006 and 2001. Inline number 1654.

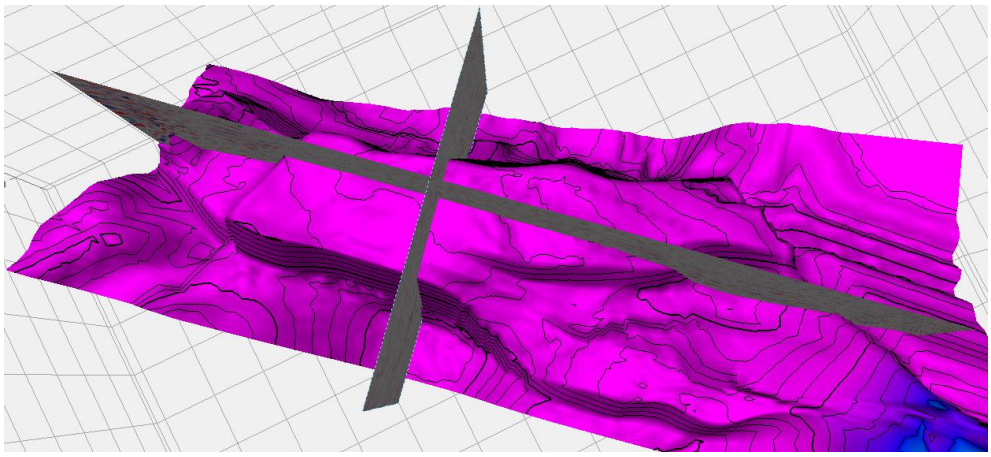

Figure 8: Norne top surface with crossline 1089 and inline 1654 of the time-lapse seismic.

3 History Matching

Reservoir models are the essential tool of a reservoir engineer, which is meant to provide predictive capacity. Therefore, it is important to optimize the models, in such a way that it epitomizes the subsurface fluid system. This is done through a history matching process. Schlumberger (2012a) defines history matching as the act of adjusting a model of a reservoir until it closely matches the past behavior of the reservoir. Initially, a geological reservoir model is created based on the known information - depositional environment, stratigraphy, geostatistically calculated rock properties, seismic response data and well measurements. The initial geological model will then be subject to fluid flow simulations, and the simulated behavior is compared to the historical production and pressure data. The model and corresponding parameters are then adjusted to produce data that resembles the historical data in a good manner. Adjustments and comparison between historic events and the model's behavior are done iteratively. After the iterative process the model is regarded as fitted and future production and drainage of the reservoir are predicted from this model.

Traditionally, history matching has been a manual process where a reservoir engineer had to manually change the parameters of the reservoir model, run the simulations and process the solutions. University students still learn this method of working, but this is mainly because it gives an understanding of how the different parameters affect the fluid flow in the reservoir. With the increasing computing power in the industry, a semi-automated approach is increasingly utilized.

Semi-automated, or computer-aided, history matching is performed by simulating the behavior of the reservoir with initially guessed reservoir parameters, then allowing the computer to run the simulation iteratively with more correct parameters until a fitted model is produced. Estimates of each iterated realization is computed through the use of an objective function that represents the model's error. The normal workflow or dataflow of a semi-automated history matching process can be illustrated as in fFigure 9.

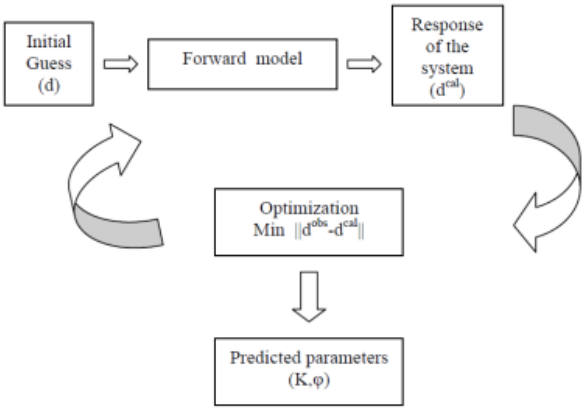

Figure 9: Common history matching algorithm (Dadashpour et al., 2007)

The algorithm can be summarized as;

1. Make an initial guess of reservoir parameters
2. Forward model the system with the guessed parameters
3. Calculate the objective function of the realization.
4. Calculate the objective function value
5. Compare the objective function value to a set convergence criteria, and;
    a. If the criteria is not met:
        Alter the reservoir parameters to minimize the function, and return to step 2.
    b. If the criteria is met:
        Algorithm has found the parameters that result in the optimum objective value.

The fitted model is used to predict the future behavior of the reservoir. Prediction can be done to the model before it has reached a fitted state, but the history matching process improves the stability, accuracy and reliability of the model.

However, history matching does not have a unique solution and the fitted model should be used with caution. History matching is an inverse problem – the solution is known and the problem is finding the underlying parameters that reproduce the known solution. The process of solving inverse problems includes a set of mathematical techniques for relating observations to an assumed model to estimate the unknown model parameters. Inverse problems are under-constrained, so they have multiple equally correct solutions. Inverse problems occur in many other science branches, like medical imaging, astronomy and acoustic tomography, and in a large extent in applied geophysics. Locating the source of an earthquake, AVO-analysis, finding gravity anomalies are all inverse problems.

From the outline of the history matching algorithm, it is possible to see that there are some components that need to be looked into. These are the forward model, objective function and the optimization procedure.

3.1 Forward modeling

To deduce the behavior of the reservoir, we need to establish a reservoir model. Geologists create geological models based on the geological knowledge of the reservoir surroundings, property data from wells and the initial 2D or 3D seismic surveys of the field. An up-scaled version of this model serves as the static foundation for the simulations of, evaluation of and decision making processes for the future reservoir production. The dynamic behavior of the reservoir has to be predicted by a forward model.

A forward model is based on fundamental physical laws and is used to convert known or guessed system parameters into a forecast of an actual physical system. In reservoir simulation, the forward model is based upon a series of laws and principles that governs fluid flow in a porous medium. Among them are:

- Darcy's equation
- Mass conservation law
- Relative permeability and capillary pressure relationships
- Equation of state

Together, they form a system of differential equations and matrices that represent the dynamic behavior of the fluid flow system. Several fluid flow simulators that utilize this system have been developed by scientists and oil companies in the past. These are based on the same physical principals, but the implementations differ in design, functions, precision and assumptions.

3.2 Objective Function

Objective functions are used to quantify the error between the compared data sets. The value of the objective function represents the total mismatch. The process of history matching seeks to minimize the mismatch, hence minimize the objective function. The function is often expressed as a least-squares formulation, which is also common in other minimizing procedures. This formulation tries to minimize the sum of the squares of the residuals, r, from the

comparison between computed and observed values. Optimum is found when the method reaches the minimum of the sum;

$$F = \sum_{i=1}^{n} r_i^2 \tag{3-1}$$

where the residual r is written as;

$$r_i = p^{obs} - p^{calc} \tag{3-2}$$

where p^{obs} is the value of the observed data and p^{calc} is the value of the simulated data. This is the general structure of the least-squares formulation, while a more specific version is usual in history matching;

$$F(m) = \frac{1}{2}(p(m) - d)^T W(p(m) - d) \tag{3-3}$$

where m is the reservoir parameters and W is a weight matrix that is used to weigh the data entries and correct for measurement errors and potential data correlations. It is supposed to be adequate to express the weight matrix as the inverse of the covariance matrix, $W = C^{-1}$.(Gosselin et al., 2003)

3.3 Optimization

History matching is essentially a minimization procedure. The concrete minimization is done by executing an optimization algorithm with the objective function as the minimizing entity. There exists numerous different optimization algorithms, but they all share the same general workflow – iteration of the forward model with successive approximation of the unknown parameters. These algorithms will seek out the local or global minima of the complex simulation model. Global optimizers are most desired, but they suffer from the need to execute numerous iterations to find the global optimum.

Optimization algorithms can be divided into two categories based on the need for calculating gradient information. The algorithms that do not utilize gradients are solely looking at the value of the objective function in their minimization.

3.3.1 Gradient methods

Gradient methods are often the most efficient optimization algorithm, but they require the calculation of derivative information. These

calculations are costly, and the function in question may be difficult or impossible to differentiate.
The gradient of the objective function is defined as:

$$\nabla F = \left(\frac{\partial F}{\partial x}\right)^T \tag{3-4}$$

There exist several different approaches for computing the gradients. (Dadashpour, 2009) mentions three of the most important ones as:

- Direct Method,
- Perturbation Method,
- Adjoint Method

For further reading about these methods, see (Dadashpour, 2009). In later years a new alternative method has been developed:

- Streamline derivation

After computing the gradients of the function, gradient based optimization methods have to be applied. Gradient Algorithms that uses the derivative information of the function include Gauss-Newton, Conjugate Gradient and Steepest Descent. For a basic applied procedure for the Gauss-Newton method, see (Dadashpour, 2009, p.85). The alternative approach of using streamlines is explained in (Dale Bakkejord and Rosseland Knutsen, 2009).

3.3.2 Derivative-free algorithms

The derivative-free methods are the methods that do not require the gradients of the function. Calculation of gradients is costly and these methods should be faster that the gradient methods, but they are not. This is because of the increase in function calls that has to be executed instead, and the inclusion of fluid flow simulations in the iteration demands high computational effort. There exist both methods that look for local optimum, as well as methods that search for global optimum. In the category of methods that find local minimum are Nelder-Mead, Trust Region Method and Hooke-Jeeves Direct Search. These methods will not be discussed. Among the methods that search for the global minimum are Evolutionary algorithms (Evolutionary Algorithm and Genetic Strategy), Simulated Annealing method and Particle Swarm Optimization.

Evolutionary algorithms are explained in (Nygaard, 2012) and use of Ensemble Kalman Filter, EnKF, is explained in (Skjervheim et al., 2005), (Szklarz, 2010) and (Begum, 2009).

3.3.3 SimOpt optimization

SimOpt uses the Levenberg-Marquardt algorithm, which is a combination of the Newton method and a steepest descent scheme. Denoting the vector of the current parameter normalized modifier values as v^k, then the algorithm estimates the step, $dv^k(\mu)$, required to minimize the objective function as:

$$dv^k(\mu) = (H + \mu I)^{-1} \nabla f(v^k) \tag{3-5}$$

where the Hessian matrix, H, is the matrix of second derivatives of f and I is the identity matrix.(Schlumberger, 2012b) The Hessian matrix is a square matrix filled with all second order partial derivatives of the function, which equals the Jacobian of the derivatives of the objective function(Weisstein, 2012);

$$H(F) = J(F') = \begin{bmatrix} \frac{\partial^2 F}{\partial x_1^2} & \frac{\partial^2 F}{\partial x_1 \partial x_n} & \cdots & \frac{\partial^2 F}{\partial x_1 \partial x_n} \\ \frac{\partial^2 F}{\partial x_2 \partial x_1} & \frac{\partial^2 F}{\partial x_2^2} & \cdots & \frac{\partial^2 F}{\partial x_1 \partial x_n} \\ \vdots & \vdots & \ddots & \vdots \\ \frac{\partial^2 F}{\partial x_n \partial x_1} & \frac{\partial^2 F}{\partial x_n \partial x_2} & \cdots & \frac{\partial^2 F}{\partial x_n^2} \end{bmatrix} \tag{3-6}$$

4 Seismic History Matching

Seismic history matching is an extension of the history matching process. In addition to minimizing the error between observed and simulated production data, seismic history matching tries to minimize the error between seismic reflections of the reservoir with the reflections of the reservoir model. Alterations of the process' components and to the work flow needs to be done to incorporate the seismic dimension, and these changes will be discussed.

The nature of the available data; production data, well data and seismic data, are fundamentally different. Production data is direct measurements of the behavior of the entire reservoir as a unit – it is only possible to infer something about the volume and content of the reservoir. Well data are also direct measurements, but direct measurements of reservoir parameters in single points. It is precise in points, or columns, of the reservoir, but the parameters in between the points are still unknown. Quite the opposite is true about the seismic data. It has data points for the entire reservoir, even in between the wells, but the resolution and certainty of the data is low, compared to well data. The seismic data do not need any correlation, because it is representative of the whole reservoir.

Alterations of the forward modeling of the reservoir include the introduction of fundamental laws and relations that govern the reflection response from the subsurface geological layers and the reservoir rocks, as well as laws that relate the reflections to reservoir properties like pressure and saturation. Among them, we find:

- Gassmann equation
- Hertz-Mindlin model
- Seismic reflectivity modelling theory

These principles form the basis for a Petro Elastic Model or PEM. PEM is the bridge between seismic and reservoir properties. It is used in both forward modeling of the reservoir properties into seismic properties and inverse modeling of seismic readings into reservoir properties. Seismic data

Seismic data is recordings of elastic waves traveling through the subsurface. These waves has to be sourced by a natural force, like an earthquake, or by

4.1 New objective function

With the introduction of seismic data into the history matching procedure, the need for a method to determine the relative influence of the production data match and the seismic data match arises. This is due to the fact that a good match between simulated and observed seismic data does not implicate a good production data match, and vice versa. The chosen methodology is probably the simplest one, weighting factors. The total objective function for the history matching simulations is assigned two decimal values that act as weights of the production and seismic mismatch function. We end up with the following expression for the total objective function:

$$F(m) = \alpha \cdot F_{prod}(m) + \beta \cdot F_{seis}(m) \tag{4-1}$$

where α and β are weights that controls the relative effect of the two contributors, and

$$F_{prod}(m) = \frac{1}{2}(p(m) - d)^T W_p (p(m) - d) \tag{4-2}$$

$$F_{seis}(m) = \frac{1}{2}(s(m) - e)^T W_s (s(m) - e) \tag{4-3}$$

where s(m) is the simulated seismic data and e is the observed seismic.

The weights are important when the quality or reliability of the factors is imbalanced. If the seismic data is coarse and strongly interpolated the weight factor, β, could be decreased to devalue the seismic mismatch relative to the production mismatch. Conversely, if the seismic data has a high resolution and reliability the weight factor could be increased to accentuate the seismic mismatch in the total objective function.

Another weighing method is described in (Aanonsen et al., 2003), where it is stated that the relative influence of the seismic data and the production data can be balanced on the basis of the sum of the inverse of the data and model error covariance matrices.

4.2 Repeatability

An important aspect of the acquisition of time-lapse seismic data is the extent of repeatability of the seismic surveys. Repeatability is a measurement of the expected variability between the base survey and the later monitor surveys. This variability is noise that affects the

quality of a time-lapse analysis, and can be caused by many different sources; setup of the source and receivers, shot count and frequency weather, tide and waves, platforms, vessels and more. Some of these noises could be eliminated, or at least minimized, while others are irrepressible. The production and injection of fluids are affecting the seismic survey in the same manner as the other sources of variation, and can therefore be regarded as noise as well. The intention of time-lapse surveying is to monitor the production effects. Therefore, it is important that there is no other effect that overshadows the production effect, and this is quantified by repeatability measures.

To assess the repeatability of a field surveying system, it is possible to perform a "zero-time repeatability test", which is described by Ross and Altan (1997). The test includes performing a monitor survey in quick succession to the base survey with the same setup, crew and vessels as the base survey. If the period between the two surveys is short enough, so that production effects are negligible, the resulting time-lapse analysis displays the non-repeatable noise. If the residual energy is small, one would expect to be able to perform high quality time-lapse analyses of the production effects.

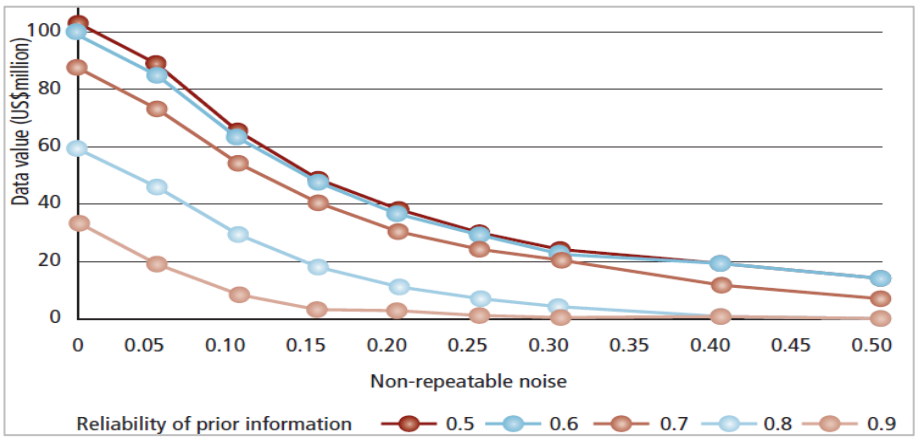

Figure 10: The value of the acquired data decreases with increasing amount of non-repeatable noise (Houck, 2007)

The value of a time-lapse survey is dependent on the repeatability. Figure 10 shows the effect of a monitor survey on the value of an imagined drilling program. The added value to the project decreases when the amount of non-repeatable noise increases, or in other words, the repeatability decreases. In the same figure, it is

also observable that the value of additional seismic data is dependent on the reliability of prior information.(Nygaard, 2012)

4.3 Petro-elastic modeling

In the event of including seismic data in the otherwise seismic-free history matching procedure described in chapter 3, it is essential to introduce a petro-elastic model. The petro-elastic model, PEM, serves as the nexus between fluid and rock properties, that govern fluid flow in porous media, and the elastic and seismic properties, that govern wave propagation in the same media. This link has to be traversed to obtain data in comparable domains, either in a forward modeling of the properties of the reservoir model or in an inversion process of the observed seismic data. This makes it possible to simulate the seismic response of the underground based on the simulations of the behavior and state of present fluids and the depletion of pressure.

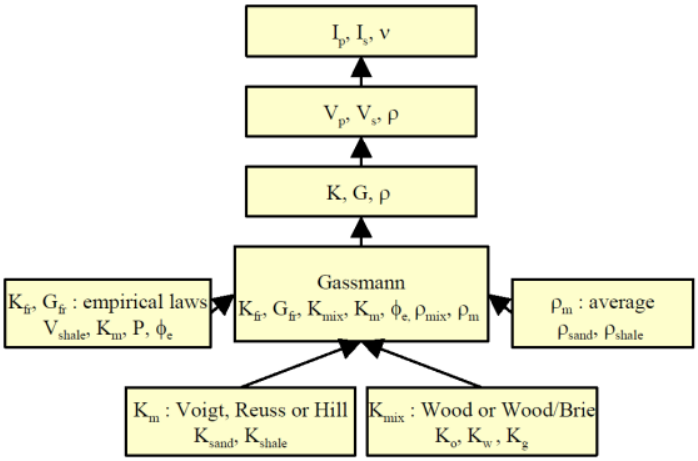

Figure 11: PEM simplified workflow(Gosselin et al., 2003)

The PEM itself is a set of equations and empirical laws calibrated to core tests and laboratory experiments, which relates elastic properties, like wave propagation velocities, acoustic impedance and density, to fluid and rock properties, like pore pressure and fluid saturation. The PEM workflow for forward modeling of reservoir properties, like permeability and porosity, into seismic properties, like wave velocity and acoustic impedance, is illustrated in Figure 11.

4.3.1 Mathematical background

The most fundamental seismic relationship that affects the seismic surveying of the underground is the speed of wave propagation. The waves generated by, in an offshore setting, an air gun, propagate through the subsurface with a speed that relies on the elastic properties of the medium in which they propagate.

Originating in the aforementioned air gun blast is both pressure waves and shear waves. They differ in the direction of vibration compared to their direction of propagation - pressure waves, or P-waves, are longitudinal, while shear waves, or S-waves, are transverse waves.

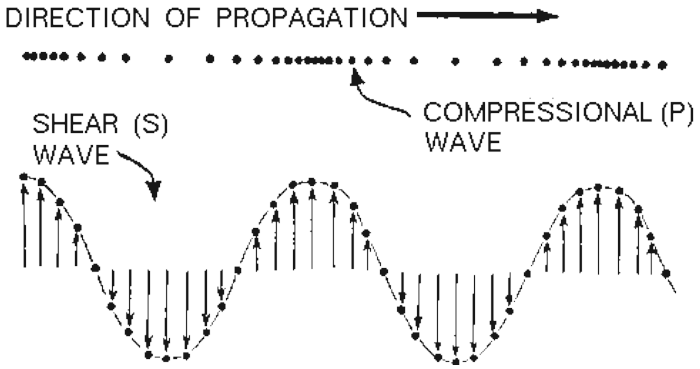

Figure 12: The propagation and particle motion of pressure and shear waves(USGS, 2012)

The two wave types has the same origin, but is affected by the elastic properties of the propagation medium in a slightly different way. Together, speed measurements of both wave types give more information about the underground. The propagation speed of pressure waves can be expressed as:

$$V_P = \sqrt{\frac{K + \frac{4}{3}\mu}{\rho}} = \sqrt{\frac{\lambda + 2\mu}{\rho}} \tag{4-4}$$

Where K is the bulk modulus of the wave propagation medium, μ is the shear modulus, λ is Lames first constant and ρ is the calculated volume average porosity of the solid and liquid phase of the traversed medium. Shear waves is not affected by changing bulk modulus and can be expressed as:

$$V_S = \sqrt{\frac{\mu}{\rho}} \tag{4-5}$$

The most important difference between the propagating ability of the two wave types is that shear waves are not capable of traveling through fluids, as the shear modulus of a fluid is zero. To be able to record both wave types, listening cables has to be installed on, or dragged across, the ocean bottom. Permanent installation of listening cables by burying them down in the subsurface on top of reservoirs is an expanding feature of resource development. It has been done on large fields, like Valhall (Lane et al., 2006) and Ekofisk (Tolstukhin et al., 2012).

Finding the travel times through propagation speed calculations could be easy in an ideal situation with an isotropic and linearly elastic medium. This is seldom the case and further calculations have to be done in order to determine these properties. Falcone et al. (2004) describes the problem of stiffening in a saturated medium. The process makes it hard to calculate the moduli. The phenomenon occurs as pressure waves pass through a saturated medium and creates local gradients of pressure that stiffens the combined solid and liquid phase. The most common approach of overcoming this problem is the fluid substitution theory of Gassmann (1951).

Gassmann's equation relates the bulk modulus of a porous medium saturated with hydrocarbons to the porosity of the medium and the bulk modulus of the fluids and the surrounding matrix rock. The relationship is stated as:

$$K = K_{dry} + \frac{\left(1 - \frac{K_{dry}}{K_s}\right)^2}{\frac{\phi}{K_{fluid}} + \frac{1-\phi}{K_s} - \frac{K_{dry}}{K_s^2}} \tag{4-6}$$

and

$$\mu_{sat} = \mu_{dry} \tag{4-7}$$

where K_{sat} is the effective bulk modulus of the saturated medium, K_{dry} is the bulk modulus of the fluid-free frame mineral, K_s is the bulk modulus of the porous matrix and K_{fluid} is the bulk modulus of the fluids present in the rock. Φ is the effective porosity of the medium and μ_{sat} is the corresponding shear modulus of the saturated rock and μ_{dry} is the shear modulus of the rock in a dry state. The equation is based on assumptions about the homogeneity of the modulus of the rock minerals and statistical isotropy of the pore space. It is also limited to cases where the wave frequency is sufficiently low such that there is sufficient time for the pore fluid to flow and eliminate

any wave-induced pressure gradients. The more general equations for wave propagation in a poroelastic medium are the Biot's equation - Gassmann fluid substitution is the lower frequency limit of Biot's equation.

Batzle and Wang (1992) presents their findings about the seismic properties of pore fluids. They found that the properties of pore fluids, like density, viscosity, velocity and bulk modulus vary substantially but systematically under the pressure and temperature conditions that is typical of oil exploration. In their paper, Batzle and Wang explain several equations that relate pore fluid properties to seismic properties. Among them is an equation of the bulk modulus of brine with dissolved gas, as

$$K_G = \frac{K_B}{1 + 0.0494 R_G} \tag{4-8}$$

Where K_B is the bulk modulus of gas-free brine and R_G is the gas-water ratio at room pressure and temperature. For more details and other fluid-seismic relations see the referenced paper. Other authors, like Hashin-Shtrikman, Hertz-Mindlin and Gardner have also presented relevant research about the relation between seismic properties and fluid and rock properties. Further reading is recommended, as these have not been explored by the author.

In practice, the elastic property that is used to map the lithography of the subsurface is often the acoustic impedance. Acoustic impedance, Z, is the product of the propagation speed, V, and the density of the medium, ρ, and can be expressed simply as:

$$Z = V * \rho \tag{4-9}$$

Seismic waves propagate away from the source until they reach a property interface with a distinct difference in elastic properties. These interfaces are mapped in a seismic interpretation process to map the lithology, because they represent the border between lithotypes. Acoustic impedance can be correlated to rock properties through rock physics relationships, such as those of Batzle & Wang and Gassmann.

The lithology interfaces, the variations in acoustic impedance that are spotted through the recorded seismic reflections are a combination of response changes that are induced by both saturation and pressure changes. Seismic reflectivity of the porous medium under depletion is influenced by two simultaneous effects; pressure

drop and saturation fluctuation. The petro-elastic model has to account for both of these. These effects are measured independently of each other in a well – the effect on the acoustic impedance from pressure change and saturation changes have to be decoupled by well data.

5 Application to Norne

History matching has been applied to Norne since the first oil was produced from the first well. The act of including time-lapse seismic data in the matching loop has also been thoroughly experimented with and applied in the actual reservoir management process.

First, the seismic data that is available from the field is presented before the act of weighting the seismic data relative to the production and well data is discussed. Then the zonation and the chosen matching parameter are depicted and the details of the explicit application of a petroelastic model are described.

5.1 Seismic data available

Statoil has made available additional elastic data for the Norne field on the request of the author - seismic cubes of relative change in acoustic impedance. The cubes have been corrected for time shift between vintages individually and then subtracted from each other to establish the time lapse difference. To adapt the seismic data to the reservoir model the cubes have been depth converted, and then exported in Seg-Y format with IBM float values.

The observed survey data format needed for seismic history matching with SimOpt requires the absolute change in acoustic impedance, not the relative change in percentage of base value. The data had to be converted to absolute values. This process was done using Petrel and MatLab.

5.1.1 Conversion to absolute change

The relative change in acoustic impedance can be defined as:

$$A_{rel} = \frac{A_2 - A_1}{A_1} \tag{5-1}$$

where A_1 is the acoustic impedance of the base survey and A_2 is the acoustic impedance of the monitor survey. Then, if we assume that we can approximate A_1 as the simulated impedance of the simulation model, we can calculate the absolute change of acoustic impedance as:

$$A_2 - A_1 = A_{rel} \times A_1 \tag{5-2}$$

and A_2-A_1 is used as input in SimOpt.

The first challenge with this approach is the different scaling of the data sets. The relative changes is of seismic resolution – a regular grid with grid cells of 12.5x12.5x4m, while the simulated acoustic response of the simulation model at the base survey time has values for each grid block of the reservoir model, with unregular grid blocks of 100x100x25m. The wanted SimOpt input with absolute changes in acoustic impedance has to be of reservoir grid resolution. The observed relative changes have to be rescaled to the reservoir model grid.

The rescaling of the survey data was done using geological modelling in Petrel. The process was run with seismic resampling, intersection and harmonic average as properties, which means that the seismic data was resampled by weighting and comparing all seismic values that is present in each reservoir block. These samples went through a harmonic averaging filter first, resulting in a value for each reservoir grid block. The resulting property map can be seen in fFigure 13.

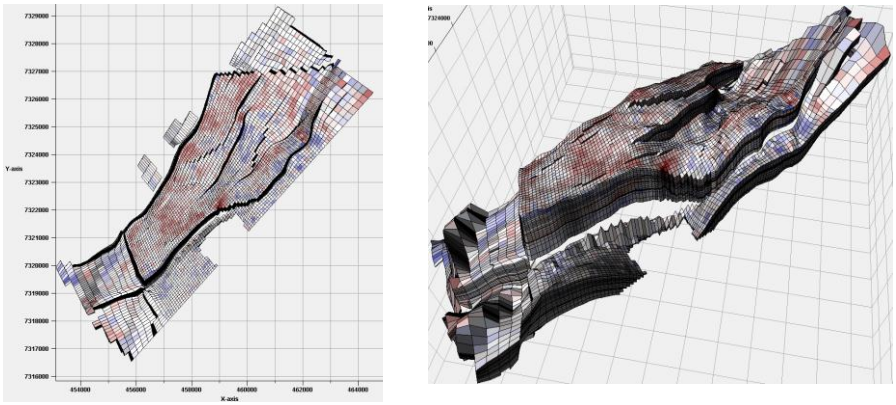

Figure 13: Seismic property map of relative change in acoustic impedance. Two-dimensional top layer map to the left and three-dimensional map to the right.

This seismic property was then exported in SimOpt observed data format. The acoustic impedance of the simulation model from time step 1. August 2001 was also exported in the same way and both files were read into Matlab. The value of the seismic property in a given grid block was multiplied to the value from the same block of the data with simulated impedance values, following equation *(5-2)*. This was done for all grid blocks, and the resulting value matrix was written to a SimOpt observed survey format as seen in Appendix A:

The author was not successful in calibrating the seismic data in an optimal manner, and the discrepancy of the seismic data is huge

compared to the production data. This causes this thesis to look at relative differences, rather than which weighting factor combination provides the closest fit.

5.2 Weighting factors

Weighting of the different data-types is needed to balance their contribution to the matching process, and also to avoid over-fitting the data. (El Ouair et al., 2005)

(Gosselin et al., 2001) show that an initial auto-balance between the production and seismic data sets leads to an enhanced global history match. They suggest basing the weighting coefficients on the initial seismic and production discrepancies. If the initial seismic mismatch is twice that of the production data, the weights in equation (*4-1* should be altered so that $\alpha = 2*\beta$. This is meant to provide a better convergence of the matching process. (Harb, 2004) has explored different ways of implementing this - only one of them will be tested in this thesis, in chapter 6.5.

5.3 Region Zonation in SimOpt

(Morell, 2010) undertook the mission of history matching the Norne field in his master thesis in 2010. He first did a conventional manual history matching, before he used SimOpt to do the same matching in a semi-automatic way. One of the history matching strategies used by Morell was to attempt to control the water rise of the model. The carbonate barriers had to be altered for the observed water rise to take place – local vertical transmissibility changes was done in layers 11, 12 and 15. These areas are shown in fFigure 14.

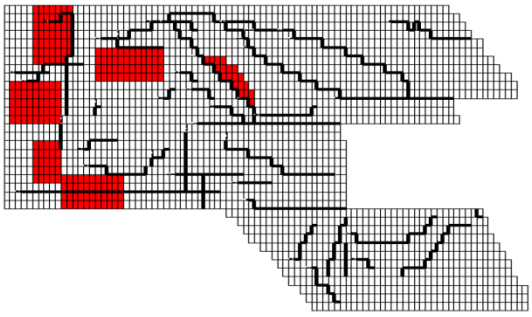

Figure 14: Regions for modifying vertical transmissibility to control water rise(Morell, 2010)

Morell altered the transmissibility in these regions to ten times the original value in order to allow the water to rise as observed. He also opened the simulator's possibility of altering the vertical transmissibilities below the producing wells. This was done to benefit the well match – especially water cut.

The applied region zonation can be seen in fFigure 15. In addition to the water rise modifier for the red region, two other regions were utilized in the history matching. The blue regions are the trajectories of the wells that produce too much water, while the green regions are the trajectories of the wells that produce too little water. Both well trajectory regions are given an initial value modifier of 1, but they are given the possibility to change between 0.1 and 100. These regions are vertically extended in all layers beneath the closest well.

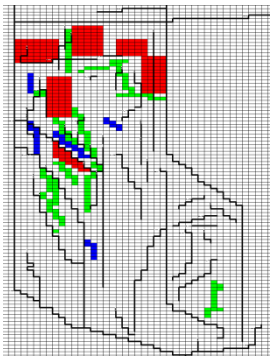

Figure 15: Applied region zonation for SimOpt automatic history matching. Red areas are holes in the carbonate barrier. The green area is the trajectory below the wells producing too little water, and the blue areas are the trajectories below the wells producing too much water.

5.4 Petro-elastic model

The petro-elastic model of the Norne field has been developed specifically to fit the reservoir and the present rocks and fluids there. As a part of the Norne database, Dadashpour (2012) has summarized the important parameters and properties for both fluids and frame rocks. This can be seen in tTable 3.

Shale properties			
Shale Type1 (Inside reservoir-Not Formation)	P-wave Velocity S-wave Velocity Shale Density	V_{PSH1} V_{SSH1} ρ_{SH1}	3200 m/s 1600 m/s 2300 kg/m^3
Shale Type 2 (overburden)	P-wave Velocity S-wave Velocity Shale Density	V_{PSH2} V_{SSH2} ρ_{SH2}	3350 m/s 1800 m/s 2450 kg/m^3
Shale Type 3 (Under reservoir)	P-wave Velocity S-wave Velocity Shale Density	V_{PSH3} V_{SSH3} ρ_{SH3}	3500 m/s 1900 m/s 2450 kg/m^3
Rock (Sand) properties			
Garn formation (Layer 1 - 3)	Frame bulk modulus Frame shear modulus Matrix bulk modulus Matrix Density	k_{fr} k_{fr} k_{ma} ρ_{ma}	18.8-36.8φ 11.8-21.4φ 37 GPa 2650 kg/m^3
Ile,Tilje, Tofte Formations Layer (5 -22)	Frame bulk modulus Frame shear modulus Matrix bulk modulus Matrix Density	k_{fr} k_{fr} k_{ma} ρ_{ma}	18.5-27.4φ 10.9-13.0φ 37 GPa 2650 kg/m^3
Fluid properties			
Fluid bulk modulus (Reservoir Temperature 98.3 C) Oil density Water density Water salinity Gas density		k_o, k_w, k_g ρ_o ρ_w SAL ρ_g	From Batzle and Wang * 860 kg/m^3 1000 kg/m^3 0.05 ppm 190 kg/m^3

Table 3: Model of input parameters for the petro-elastic model for the Norne field (Dadashpour, 2012)

The Norne reservoir consists of sandstone and shale – two rock types with very different properties. Jurassic sandstone is the hydrocarbon bearing rock type, while the sealing Not formation is a shale layer in-between the reservoir sandstone layers. Shale is also surrounding the reservoir – both the overburden and the lithotype below the reservoir are shale-based.

Wave propagation velocity for the shale areas are reported, as well as the density. Density, shear modulus and bulk modulus are the properties that are included in the petro-elastic model. Together, these values build a foundation for calculating the seismic response of the subsurface rocks. To complete the petro-elastic model and include the effect of hydrocarbons and water, also properties of the fluids need to be incorporated. The bulk modulus and density of each present fluid and the salinity of water are the relevant properties of the fluids. Fluid bulk modulus is calculated using the equations and assumptions of Batzle and Wang (1992), while the salinity and density values are averages of values of the fluids-in-place.

5.4.1 PEM in Eclipse

The utilized fluid flow simulator, Schlumberger's Eclipse, has a petro-elastic model option. Simulation properties of the rocks and fluids of the reservoir are used to calculate the acoustic response of both the rocks and fluids, which is combined for the calculation of the total acoustic response. Each grid cell is assigned a response value.

Fahimuddin (2009) describes in detail the procedures and underlying equations and assumptions in the petro-elastic model of the Eclipse simulator.

The effective pressure, P_{eff}, is calculated from the pore pressure, P_{pore}, and the overburden pressure, P_{over}. For the Norne reservoir, effective pressure is calculated directly from the true vertical depth:

$$\begin{aligned} P_{eff} &= P_{ext} - P_{hyd} \\ &= (0.0981 * (9 \times 10^{-5} * TVD + 1.7252) \\ &\quad * TVD) - P_{hyd} \end{aligned} \tag{5-3}$$

The mineral bulk modulus, K_S, is calculated through a polynomial function that relates it to the effective porosity, φ_{eff}.

$$K_S = C_0 + C_1 \, \phi_{eff} \tag{5-4}$$

C_0 and C_1 are constants found in the calculation of the effective bulk modulus of the minerals as the zeroth and first order polynomial coefficients. The shear modulus of the minerals is a direct input to the simulator model.

In (Fahimuddin, 2009), relationships and equations for dry rock bulk and shear modulus and effective pore fluid properties are outlined. Eclipse uses the standard Gassmann fluid substitution to calculate the elastic parameters, as seen earlier in chapter 4.3.1.

Eclipse 100 uses the keyword PECOEFS to read input data for the petro-elastic model calculations described in this chapter (Schlumberger, 2008a). Statoil has provided the specific values for this keyword for the Norne model and they were reported by (Morell, 2010), together with the necessary tables of bulk and shear modulus for the dry frame. All these Eclipse inputs are present in Appendix A in (Morell, 2010), and details about the keywords can be read in (Schlumberger, 2008a).

6 Results

To assess the importance and relative performance of the automated history matching in SimOpt with different weighting of the observed data sets, well logs and the seismic survey, regressional analysis was run for different weighting factor combinations.

The model was first run with only production data as matching parameters, then with only the seismic data activated. These two cases will be referred to as Case P and Case S, respectively. In regards to the weighting factors, in Case P α was set to 1 and β was set to 0. This forces SimOpt to only account for the production error, given that the error estimates for the seismic data is multiplied by zero. For Case S, the opposite weighting factors were applied - α was set to 0 and β was set to 1. In this way, enforcing SimOpt to neglect the production error, and only account for the discrepancy of the seismic survey data.

The third combination of weighting factors that were applied and tested with SimOpt was a case where both production and seismic data were included in the matching process. Both seismic and production data were weighted equally as 1, giving a case were the discrepancy of production and seismic data have an equal effect on the final and total history match result. This case will be referred to as Case SP.

The fourth and final weighting factor combinations that have been applied in this thesis work, is based on the theory about auto balancing of the weight factors which was presented by Gosselin et al. (2001) and further explored by Harb (2004). It will be explained further together with its results, and will be referred to as Case Auto.

First, the way of comparing the different cases will be explained, then the cases will be presented individually and, finally, a comparison of the cases will be presented.

6.1 Comparison parameters

SimOpt uses root mean square values or RMS for short, as the measurement scale for the fit and quality of the history match. The index that is reported from the software is formed from the regression objective function and is expressed as:

$$RMS = \sqrt{\frac{2f}{m}} \tag{6-1}$$

where m is the total number of observations over which the index is formed, and f is the objective function. (Schlumberger, 2012b) The total RMS for the global domain is reported, together with an RMS index for each observed data entity, that being individual well, well groups or seismic surveys.

The partial derivative of the RMS index with respect to each of the parameter modifiers is called the RMS sensitivity. These sensitivities are calculated for each observed data entity for each parameter modifier, and it indicates how the RMS index is affected by perturbations of the parameter modifiers. The sensitivity is defined as:

$$\nabla(RMS) = \frac{\nabla f}{m \times RMS} \tag{6-2}$$

where m is the number of observed data points and ∇f is the gradient of the objective function, defined as

$$\nabla f = \alpha(\nabla r)^T r + \beta(\nabla s)^T C_S^{-1} s + \gamma \cdot \nabla f_{prior} \tag{6-3}$$

where ∇r and ∇s is matrices given by

$$[\nabla r]_{ij} = \frac{\partial r_i}{\partial v_j} = -\frac{w_d w_i}{\sigma_d}\left(\frac{\partial c_i}{\partial v_j}\right) \tag{6-4}$$

and

$$[\nabla s]_{ij} = \frac{\partial s_i}{\partial v_j} = -\frac{w_d}{\sigma_d}\left(\frac{\partial c_i}{\partial v_j}\right) \tag{6-5}$$

respectively (Schlumberger, 2012b). In this thesis the prior information term, f_{prior}, has been neglected, in accordance to the decision of Gosselin et al. (2003) to do the same. Equation (6-3) will therefore lose its last term.

The Hessian matrix can indicate the condition of the regression and tell whether a parameter is well suited for the attempted history matching. If a Hessian matrix has dominant diagonal elements that are approximately equal in size, the matrix is 'good'. A 'good' Hessian is indicated by the diagonal dominance of the matrix, which is defined as:

$$\frac{\sum_{i \neq j} |H_{ij}|}{H_{ij}} \tag{6-6}$$

Parameters with a small diagonal dominance value are expected to perform better in a regression than a high value parameter. It will converge towards the solution faster – the match will be finished in fewer iterations.

6.2 Case P

The first case that will be presented is the all-production case, Case P. This is the traditional history matching, where well logs, like gas-oil ratio, bottom hole pressure and water-cut are parameters in the process.

The evaluation run of this case returned a global RMS-value of 563, with values for the individual well parameters ranging from the RMS of the water-cut of well D-1H close to 0 to the RMS of the gas-oil-ratio of well K-3H with a RMS value of 18448. A selection of RMS values can be seen in tTable 4 and the entire table of RMS values can be seen in a0together with the RMS sensitivities for all the three regions.

Table 4: A selected range of RMS values for Case P

Name	Domain	RMS
Total	GLOBAL	562,46
WGOR	K-3H	18448
WGOR	E-3AH	1175,9
WGOR	D-4AH	439,94
WBHPH	E-3AH	274,54
WBHPH	E-4AH	259,84
WBHPH	B-1BH	247,63
WWCT	E-3AH	2,3239
WWCT	D-1CH	2,1664
WWCT	D-1H	0,63037

The regressional run of Case P was automatically halted by SimOpt after four iterations. The total RMS of the fourth iteration was larger than the RMS value of the two preceding iterations. This behaviour can be seen in fFigure 16 , where the global RMS value is plotted for each iteration of the regression.

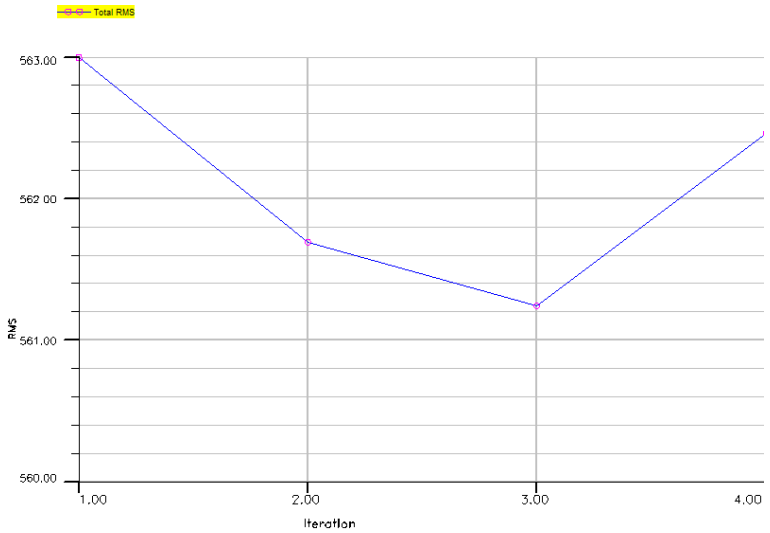

Figure 16: SimOpt RMS plot for Case P. RMS vs. number of iterations.

The simulator was not able to enhance the history matching quality much. A reduction of the global RMS value from about 563 to 561 – a change of approximately 0.35% is far from convincing. The parameters that were given to the simulator to change had only small effects on the production parameters. The simulator changed the parameters as shown in fFigure 17 . The RMS plot follows the same path as that of the Region 1 modification plot, the red line. Both of the regions that tried to alter the transmissiblities around and below the producing wells has not been altered much – indicating that the simulator assessed the gradient of these regional parameter changes as small.

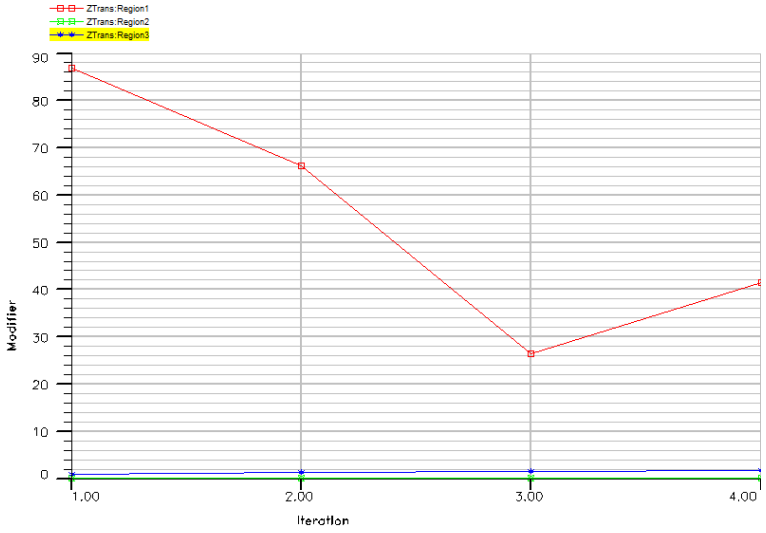

Figure 17: Parameter modifier plot for Case P. The parameter value for the three regions for each iteration. The red line indicates the development of the incremental change of the transmissibilities in Region 1. Green line indicates the changes in Region 2, while the blue line indicates the changes in Region 3.

6.3 Case S

Case S is the case where only the seismic survey data is compared to the properties of the reservoir model. The change in acoustic impedance between 2001 and 2006 is calculated from the petro-elastic modelling option of the simulator, which has been discussed in chapter 4.3, is compared to the observed survey data. Change in the acoustic impedance is therefore the only matching parameter – no well data is involved in the process.

The RMS values of Case S are easy to communicate and summarize. As there is only one observed survey data set, there is only one matching parameter – the change in acoustic impedance between 2001 and 2006. The calculated RMS for this parameter was $4.93*10^7$, as can be seen in tTable 5.

Table 5: RMS values for Case S.

Name	Domain	RMS
Total	GLOBAL	4,93E+07
dACIP	2006-2001	4,93E+07

The sudden increase in RMS value compared to Case P is due to the big error of the observed seismic data. The RMS has a declining trend, as can be seen in Figure 18. The value decreases from 49286550 to 49286150 in four iterations. This is a decrease of 400 in absolute value and about 0.008‰ of the base value. SimOpt interrupted the history match after these four iterations, indicating that it did not expect the next iteration to provide a better match.

The plot of the parameter modifications in fFigure 19, show that the simulator has not been able to find a better value for Region1 transmissibility. The simulator has tried both lowering and increasing the parameter value, but the decrease of the global RMS has not been affected. Small changes in transmissibilites in Region 2 and 3 have provided the decreasing trend. This can only mean that the parameters have minimal effect on the calculations of the change in acoustic impedance. The parameters do not cause any noticeable change in the fluid flow of the model, and they do not affect the seismic reflectivity on a field level.

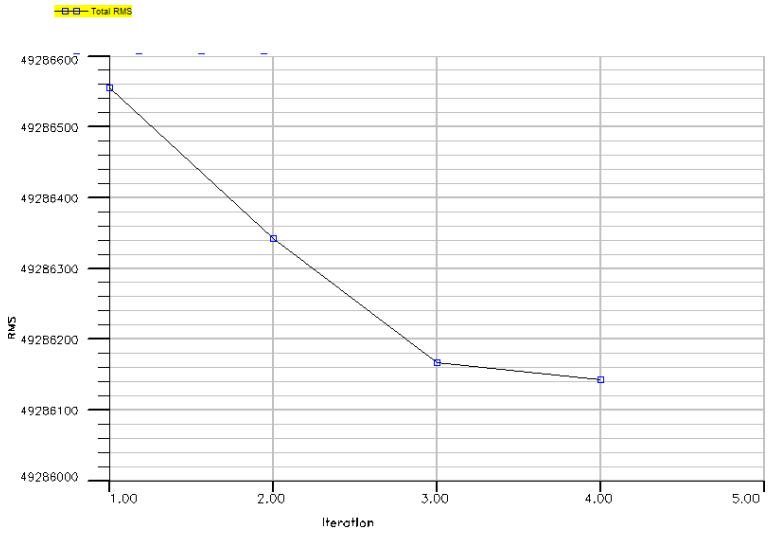

Figure 18: SimOpt RMS plot for Case S. RMS vs. number of iterations

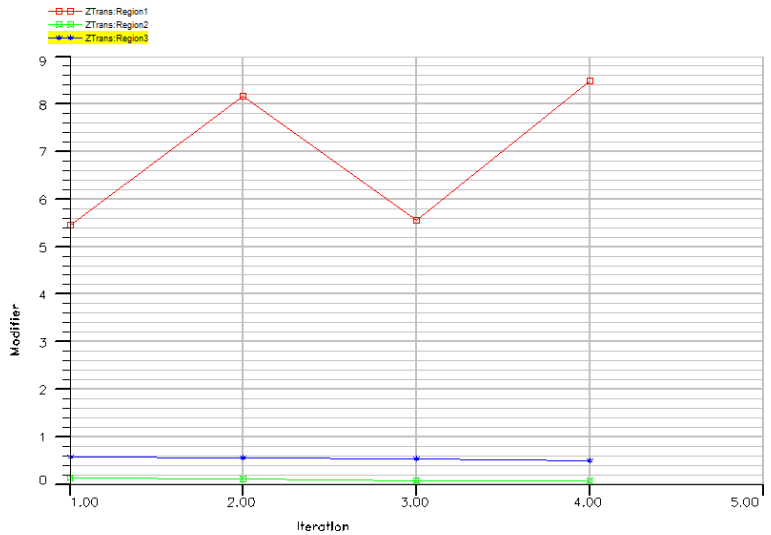

Figure 19: Parameter modifier plot for Case S. The parameter value for the three regions for each iteration. The red line indicates the development of the incremental change of the transmissibilities in Region 1. Green line indicates the changes in Region 2, while the blue line indicates the changes in Region 3.

6.4 Case SP

A history matching sequence with all parameters weighted equally is often referred to as the base case. This is the case where the production error and the discrepancy of the observed seismic data are allowed to influence the matching process with the same impact.

Figure 20: Selected range of RMS values for Case SP

Name	Domain	RMS
Total	GLOBAL	4,7426E+07
Production	GLOBAL	583,84
Survey	GLOBAL	4,9286E+07
dACIP	2006-2001	4,9286E+07
WGOR	K-3H	19200
WGOR	E-3AH	1178,1
WGOR	B-1H	335,59
WBHPH	E-3AH	274,55
WBHPH	B-1BH	241,46
WBHPH	K-3H	237,24
WWCT	E-3AH	2,3214
WWCT	D-1CH	1,7833
WWCT	E-2AH	1,6107

The seismic discrepancy and the RMS value of the well logs are in completely different value ranges. The survey data has a RMS value of $4.93*10^7$, while the production errors range from 20 000 to 1. This causes a skewed distribution of the influence on the global RMS, which is closer to the survey RMS at $4.74*10^7$. The development of the RMS in the iterative process of SimOpt can be seen in fFigure 21.

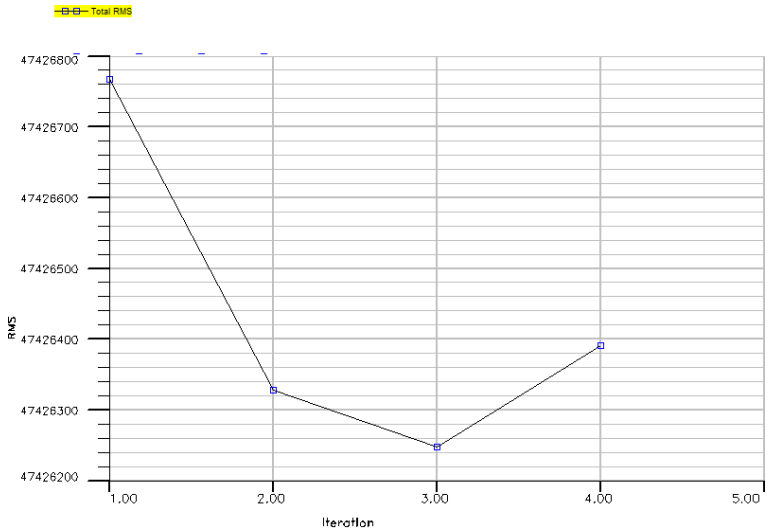

Figure 21: SimOpt RMS plot for Case SP. RMS vs. number of iterations

The global RMS has a decreasing trendline for the three first iterations, while the RMS value increases for the fourth iteration. History matching is stopped by SimOpt because of the small improvement of the first iterations, as well as the increase of RMS in

the last iteration. The parameter modifier plot seen in Figure 22, shows that SimOpt has tried to find optimal values of the parameter for all three regions. Based on the development of the global RMS and the parameter modifications, it can be concluded that the process has found an approximate best-match in the third iteration. The change of the chosen parameters has not been able to alter the quality of the history match noteworthy, and the process was halted.

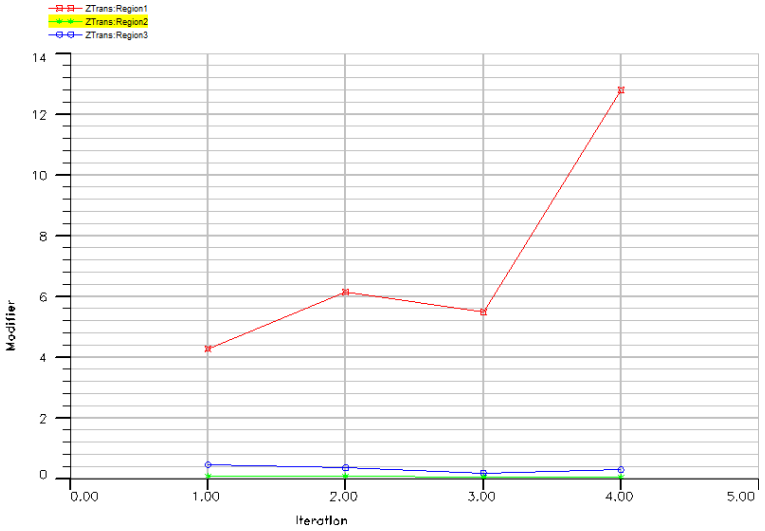

Figure 22: Parameter modifier plot for Case SP. The parameter value for the three regions for each iteration. The red line indicates the development of the incremental change of the transmissibilities in Region 1. Green line indicates the changes in Region 2, while the blue line indicates the changes in Region 3.

6.5 Case Auto

Using the relative difference between the seismic matching error and production matching error is meant to increase the quality of the history match. This was explained in chapter 5.2. In this case, the RMS values calculated in the evaluation run of the base case – Case SP, the case with equal weighting of production and seismic. Since the seismic data discrepancy is large and the original match of production data is relatively well-matched, the ratio between seismic RMS and production RMS is also large. The ratio was calculated as:

$$\frac{Seismic\ RMS}{Production\ RMS} = \frac{4{,}7426E+07}{583{,}84} \approx 84400 \tag{6-7}$$

which leads to the following weighting coefficients; $\beta = 1$ and $\alpha = 84400\beta = 84400$.

The balanced weighting coefficients cause the survey discrepancy and the well log errors to be in the same value range.

This may be a good starting point for the automated history matching in SimOpt. Calculated RMS values can be seen in tTable 6. The seismic RMS value is approximately the same as in the earlier cases including the seismic data, like Case S and Case SP. As the seismic data is weighted with β equal to 1, this was anticipated. The order of the production RMS values has increased with a factor of 5, as all values have been multiplied by 84400. Production RMS ranges from 1.56*109 to 30.

Table 6: Selected range of RMS values for Case Auto

Name	Domain	RMS
Total	GLOBAL	4,9155E+07
Production	GLOBAL	4,7517E+07
Survey	GLOBAL	4,9283E+07
WGOR	K-3H	1,5593E+09
WGOR	E-3AH	9,9137E+07
dACIP	2006-2001	4,9283E+07
WGOR	D-4AH	3,7177E+07
WBHPH	E-3AH	2,317E+07
WBHPH	E-4AH	2,1931E+07
WBHPH	B-1BH	2,0883E+07
WWCT	E-3AH	1,9616E+05
WWCT	D-1CH	1,8568E+05
WWCT	D-1H	5,2684E+04

Regression of the Norne model with the balancing weights implemented returns a RMS improvement as seen in fFigure 23. During the seven iterations that the simulator was allowed to run, all iterations show a better total RMS value. An absolute decrease of 270000, which is a relative change of 0.5%, was experienced at the end of the seventh iteration.

The parameters were altered by SimOpt as seen in fFigure 24. Small changes have been done to the vertical transmissibility in region 2 and 3, while the parameter for region 1 has been altered extensively. From a base value of 10, the region 1 parameter has been increased to 87 in the final iteration. As the global RMS value has decreased for the fifth iteration where SimOpt tested the implication of going back to a low region 1 parameter value, the subtle changes of region 2 and region 3 parameters have had an effect.

In chapter 5.2, the thesis work of Harb (2004) explores various methods of calculating the auto-balancing weighting coefficients. These have not been tested in this thesis work, due to the large discrepancy of the seismic data and the large difference in influence of the two dataset errors.

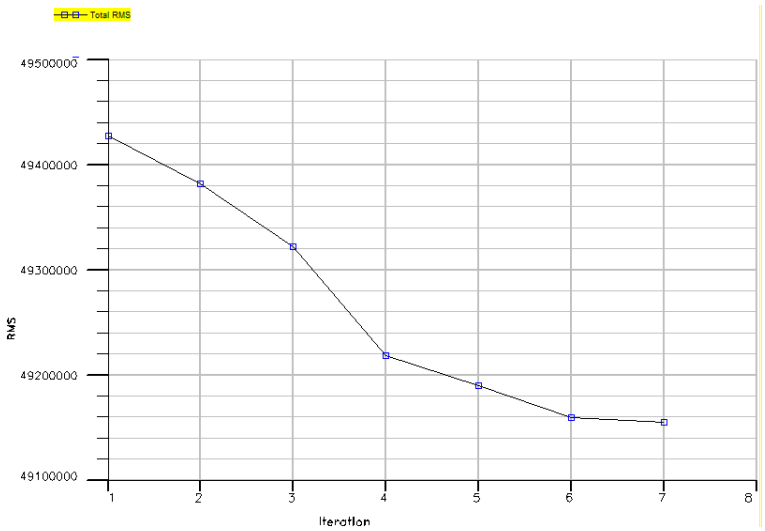

Figure 23: SimOpt RMS plot for Case Auto. RMS vs. number of iterations.

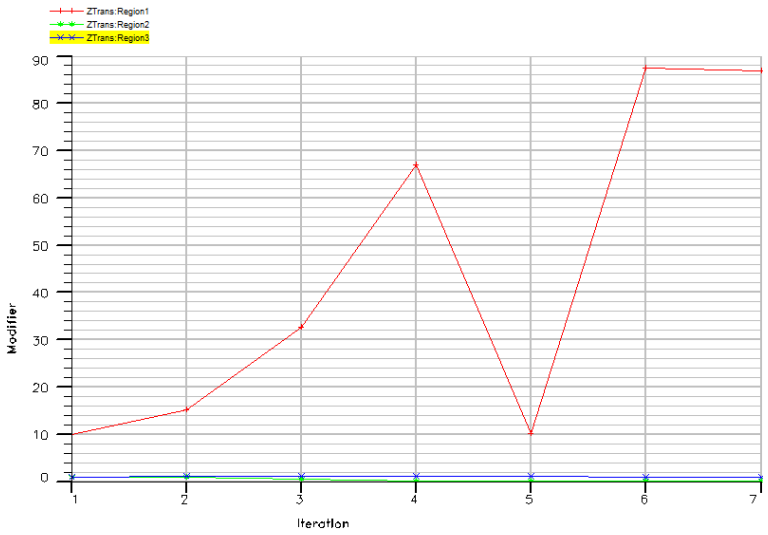

Figure 24: Parameter modifier plot for Case Auto. The parameter value for the three regions for each iteration. The red line indicates the development of the incremental change of the transmissibilities in Region 1. Green line indicates the changes in Region 2, while the blue line indicates the changes in Region 3.

6.6 Comparison of cases

The absolute RMS values in the different cases are heavily influenced by the discrepancy of the seismic survey data. Cases S, SP and Auto have all global RMS values in the same order and all include the seismic data in the history matching. If the seismic survey had been better fitted originally, RMS values for these cases would

close in on the RMS value of the pure-production case, Case P. This would instigate a much better and more correct history match.

The relative improvement calculated with the different weighting coefficient combinations are small for all cases, but they range from 0.008 per mille for Case S to 0.5% for Case Auto. Case P has a change of 0.35%, while Case SP has a change of 0.001%. The theory of auto balancing weighting coefficients seems to be confirmed in this very small test. The auto balanced case performs better than the other case, also beating Case P that has a much smaller base RMS value. In practice, the ratio between α and β in Case Auto causes the seismic data to influence the total RMS as much as the largest production RMS entities. This makes Case Auto, in practice, the true case where production and seismic are equally weighted.

All cases have a decreasing RMS plot development, but their parameter modifier plot is very different from each other. For Case Auto Region1 transmissibility modifier is increased to about nine times the original value, while the same region parameter for the other cases ends with values of about 13, 8 and 40. This shows that the final history matched model has been influenced quite a lot by the combination of weighting coefficients.

7 Discussion

Several challenges and problems with the seismic history matching process described in this thesis should be highlighted and discussed. In this chapter challenges for the data and the practical execution of the methods are discussed, and the results are further explained.

7.1 Challenges of using acoustic impedance

There are several challenges and sources of error with choosing to utilize the change in acoustic impedance in the history matching procedure.

- Side lobes in the inversion – a positive change in acoustic impedance due to e.g. water flooding will also have side lobes of negative changes above and below. Changes that is not real.
- Uncertainties related to wavelets.
- Noise in the data - the data is not based on surveys with perfect repeatability. The Norne FPSO and external sources of seismic waves and acoustic reflections will affect the results.
- Upscaling of the acoustic data to the reservoir grid.
- Uncertainties in depth conversion in the transfer to reservoir grid scale. The uncertainty of the geographical location of the acoustic reflections makes it difficult to place the changes correctly in areas near the grid cell boundaries in the grid layer.

The Statoil operating team of Norne has tried to surpass and eliminate the problem of side lobes by neglecting negative changes in acoustic impedance in cases of water flooding. In any area of the field where water flooding is an active process, all negative changes has been zeroed out. All changes in the formations Ile and Not, the top four layers of the simulation model, has been disregarded, as well as all values deeper than 10 m below the initial oil water contact. The E-segment has a pressure flank which affects the seismic data values. It causes a reduction in acoustic impedance, due to the increased pressure. These are changes that the operating team has done with the acoustic impedance data, but not something that the author has implemented in this project.

The complexity of data acquisition, survey repeatability, seismic processing and seismic inversion makes it particularly challenging to estimate the uncertainties of time-lapse seismic data. The challenge of specifying the uncertainties could be solved by performing a Bayesian inversion in the creation of the history matching data.

7.2 Practical Aspects of integrating seismic data

To be able to do a successful 4D seismic survey it is essential to have repeatable acquisition geometry, surroundings and processing. Acquisition geometry should be planned in the early phase of new field developments, so that the 4D-repeatability of the field is maximized. It is easier to establish highly repeatable acquisition geometry for an undeveloped project, where this can be emphasized from the start. However, increase of the repeatability of established fields is possible.

A feasibility and risk assessment study has to be executed prior to a 4D seismic project. It should be a staged decision-taking process with increasing technical complexity, so that a possible deal-breaker is discovered with minimal time and effort. The first step is to check the first-order critical variables in three tests:

- Is the reservoir rock highly compressible and porous?
- Is there a large compressibility contrast and sufficient saturation changes over time between the fluids to be monitored?
- Is it possible to obtain high-quality 3D seismic data in the area?

These tests should be expanded by going more in depth of the parameters. The important reservoir parameters are rock and fluid compressibility, saturation change, porosity, and predicted seismic impedance change. Important seismic parameters are seismic image quality, seismic resolution, visibility of seismic fluid contacts, repeatability of seismic acquisition, and consistency of time-lapse seismic processing (Lumley and Behrens, 1998). If the reservoir passes these tests, core samples should be analysed and synthetic seismic should be generated. If all of these tests are favourable, the project could be expected to be successful. (Nygaard, 2012)

7.3 Value of 4D data

Based on the contribution of 4D data to drilled infill wells at Norne, value of 4D was estimated to be approximately US$240 million. The

value is heavily influenced by the accuracy of the seismic data, and it is essential to provide enough resources and time to do an extensive evaluation of expected sources of error and possible remedies for these. When faced with a budget constraint and uncertainty regarding the success of individual wells, seismic data add significant value. (Pickering and Bickel, 2006)

Integration of all available subsurface disciplines and obtainable data types should be done to diminish unnecessary risks, increase repeatability and secure a maximal accuracy of the seismic data.

7.4 Choice of comparison domain

Time-lapse seismic data is integrated in the history matching process through the comparison of simulated and observed data. There are three main domains to do this comparison in.

Pressure and saturation maps: By inverting the observed seismic data to pressure and saturation maps it is possible to compare these values directly to the simulator output. This includes both a seismic inversion to elastic parameters, and an iterative inverse interpretation from elastic parameters. This domain has been used by several authors, like (Souza et al., 2011, Lumley et al., 2003, Dadashpour et al., 2007).

Seismic domain: By forward modelling the simulator output into synthetic seismic, it is possible to compare the observed seismic directly without any seismic inversion. (Sagitov and Stephen, 2012) reports that little success has been reported using this comparison domain.

Elastic parameters: Forward modelling the reservoir parameters through a petro-elastic model together with a one-time seismic inversion into elastic parameters makes it possible to compare the two data sets. This is the domain that is used in this thesis, by SimOpt and by other authors, like (Stephen et al., 2006, Aanonsen et al., 2003, Mezghani et al., 2004, El Ouair et al., 2005).

The relationship between the three domains can be illustrated as fFigure 25.

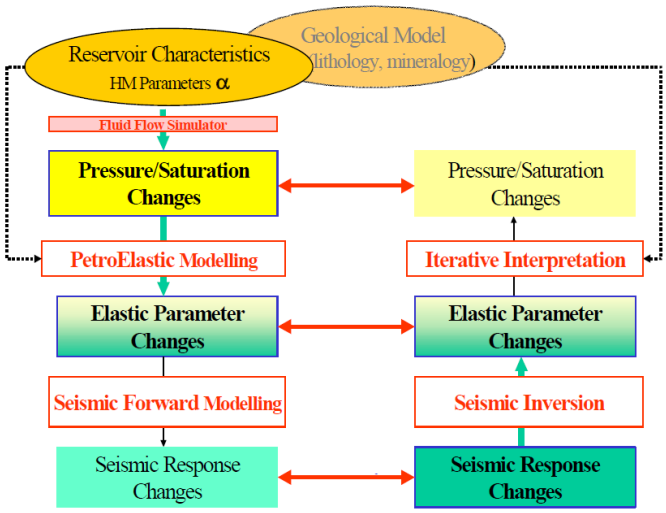

Figure 25: Seismic history matching workflow. The three comparison domains seen as red horizontal arrows. (Gosselin et al., 2003)

The benefit of using the petro-elastic domain as comparison domain is the cheap computations, because it is only necessary to do one seismic inversion in addition to the customary reservoir model iterations. The seismic history match is dependent on the data domain for comparison – different comparison domains results in different history matched models for the same base model.

7.5 Parameter choice in history matching of Norne

The parameters that were chosen to be altered by the automatic history matching process in SimOpt was gathered from the thesis of (Morell, 2010). Only vertical transmissibilities were selected, while the fault transmissibilities, also included in (Morell, 2010), was neglected. This could be some of the reason why the parameter modifier plots indicated that both Region2 and Region3 parameters never really was altered in a noticeable way.

8 Concluding Remarks

This thesis has introduced and presented the Norne field with its geology, development strategy, simulation model and the associated seismic data. The field has been described by many, as the simulation model and other engineering data have been made available to students and researchers.

History matching has been reviewed and the implementation in SimOpt, the semi-automatic history matching software used in the work of this thesis, has been discussed.

The change of objective function and the integration of a petro-elastic model have been reviewed because they are necessary to be able to integrate time-lapse seismic survey data in the optimization process.

Semi-automatic seismic history matching has been completed with different combinations of weighting coefficients. This controls the relative influence of the production and seismic data in the process. First, cases with only seismic data and only production data were done, before a case where both seismic and production data were involved as parameters in the history matching. The final case had weighting coefficients from an auto-balancing of the two separate data sets.

The auto-balanced case outperformed the other cases in regards to the improvement of fit, but the production case was superior to the others in final RMS value. This was due to the large discrepancy of the seismic data that was not possible to minimize in the time frame of this thesis work.

The most important possible improvement for any further work would be to do the same experiments with completely functioning seismic data input. Sequential weighting, weighting based on other parameters than the production and seismic survey could also be addressed.

References

AANONSEN, S. I., AAVATSMARK, I., BARKVE, T., COMINELLI, A., GONARD, R., GOSSELIN, O., KOLASINSKI, M. & REME, H. 2003. Effect of Scale Dependent Data Correlations in an Integrated History Matching Loop Combining Production Data and 4D Seismic Data. *SPE Reservoir Simulation Symposium.* Houston, Texas, USA: SPE 79665.

BATZLE, M. & WANG, Z. 1992. Seismic Properties of Pore Fluids. *Geophysics,* 57**,** 12.

BEGUM, N. 2009. *Reservoir Parameter Estimation for Reservoir Simulation using Ensemble Kalman Filter (EnKF).* Master's degree Master thesis, NTNU.

DADASHPOUR, M. 2009. *Reservoir Characterization Using Production Data and Time-Lapse Seismic Data.* philosophy doctor Thesis presented for the degree of philosophy doctor, Norwegian University of Science and Technology.

DADASHPOUR, M. 2012. Petro Elastic Model in the Norne Field. Norne Database: IO Center.

DADASHPOUR, M., LANDRØ, M. & KLEPPE, J. 2007. Nonlinear Inversion for Estimating Reservoir Parameters from Time-lapse Seismic Data. *Journal of Geophysics and Engineering***,** 13.

DALE BAKKEJORD, D. R. & ROSSELAND KNUTSEN, H. 2009. *Utilize Visualized Streamline-Derived Sensitivities in History Matching.* Master Master thesis, NTNU.

EL OUAIR, Y., LYGREN, M., OSDAL, B., HUSBY, O. & SPRINGER, M. 2005. Integrated Reservoir Managment Approach: From Time-Lapse Acquisition to Reservoir Model Update at the Norne Field. *International Petroleum Technology Conference.* Doha, Qatar: IPTC 10894.

FAHIMUDDIN, A. 2009. Petro-elastic Modeling of a North Sea Reservoir: Rock Physics Recipe and ECLIPSE Simulator.

FALCONE, G., GOSSELIN, O., MAIRE, F., MARRAULD, J. & ZHAKUPOV, M. 2004. Petroelastic Modelling as Key Element of 4D History Matching: A Field Example. *SPE Annual Technical Conference and Exhibition.* Houston, Texas: Society of Petroleum Engineers

GASSMANN, F. 1951. Über die elastizität poröser medien. *Vierteljahrsschrift der Naturforschenden Gesellschaft Zürich,* 96**,** 1-23.

GLENISTER, P. & OTTERBEIN, C. 2007. Data Processing Report for Statoil. *In:* WESTERNGECO (ed.). WesternGeco.

GOSSELIN, O., AANONSEN, S. I., AAVATSMARK, I., COMINELLI, A., GONARD, R., KOLASINSKI, M., FERDINANDI, F., KOVACIC, L. & NEYLON, K. 2003. History Matching Using Time-Lapse Seismic (HUTS). *SPE Annual Technical Conference and Exhibition.* Denver, Colorado: SPE 84464.

GOSSELIN, O., VAN DEN BERG, S. & COMINELLI, A. 2001. Integrated History-Matching of Production and 4D seismic data. *In:* SPE (ed.) *SPE Annual Technical Conference.* New Orleans, Louisiana, US: SPE 71599.

HARB, R. 2004. *History Matching Including 4-D Seismics - An Application to a Field in the Nort Sea.* Master's degree, NTNU.

HOUCK, R. T. 2007. Time-lapse Seismic Repeatability - How Much Is Enough? *Exploration & Production - Oil and Gas Review***,** 7.

LANE, H. S., KJELSTADLI, R. M., BARKVED, O. I., JOHNSON, D. T., ASKIM, O. J. & VAN GESTEL, J.-P. 2006. Constraining Reservoir Uncertainty with Frequent 4D-seismic Data at Vallhall Field. *Offshore Technology Conference.* Houston, Texas, USA: OTC 18222.

LUMLEY, D. E. & BEHRENS, R. A. 1998. Practical Issues of 4D Seismic Reservoir Monitoring: What an Engineer Needs to Know. *SPE Reservoir Evaluation & Engineering***,** 11.

LUMLEY, D. E., MEADOWS, M., COLE, S. & ADAMS, D. 2003. Estimation of Reservoir Pressure And Saturations By Crossplot Inversion of 4D Seismic

Attributes. *SEG Annual Meeting.* Dallas, Texas, USA: Society of Exploration Geophysicists.
MEZGHANI, M., FORNEL, A., LANGLAIS, V. & LUCET, N. 2004. History Matching and Quantitative Use of 4D Seismic Data for an Improved Reservoir Characterization. *SPE Annual Technical Conference and Exhibition.* Houston, USA: SPE 90420.
MORELL, E. 2010. *History Matching of the Norne Field.* Master Master thesis, Norwegian Uni. of Science and Technology.
NPD, N. P. D. 2012. Norne Factpages. NPD.
NYGAARD, S. 2012. *Seismic History Matching.* Specialization Project Report, Norwegian University of Science and Technology.
OLJEMUSEUM, N. 2013a. Norne. www.norskolje.museum.no.
OLJEMUSEUM, N. 2013b. *Petroleumskartet* [Online]. www.petroleumskartet.no. Available: http://www.petroleumskartet.no [Accessed 19. May 2013].
PICKERING, S. & BICKEL, J. E. 2006. The Value of Seismic Information. *Oil and Gas Financial Journal*, 6.
ROSS, C. P. & ALTAN, S. 1997. Time-Lapse Seismic Monitoring: Repeatability Processing Tests. *Offshore Technology Conference.* Houson, Texas, USA: OTC 8311.
SAGITOV, I. & STEPHEN, K. D. 2012. Assisted Seismic History Matching in Different Domains: What Seismic Data Should We Compare? *EAGE Annual Conference.* Copenhagen: SPE 154503.
SCHLUMBERGER 2008a. ECLIPSE 100 - Reference Manual.
SCHLUMBERGER 2008b. ECLIPSE 100 - Technical Description.
SCHLUMBERGER 2012a. The Oilfield Glossary. Schlumberger.
SCHLUMBERGER 2012b. *SimOpt User Guide 2012.2.*
SKJERVHEIM, J.-A., EVENSEN, G., AANONSEN, S. I., RUUD, B. O. & JOHANSEN, T. A. 2005. Incorporating 4D Seismic Data in Reservoir Simulation Models Using Ensemble Kalman Filter. *In:* SPE (ed.) *SPE Annual Technical Conference and Exhibition.* Dallas, Texas, USA: SPE 95789.
SOUZA, R. M., MUNERATO, F. P. & SCHIOZER, D. J. 2011. Quantitive Integration of Time-Lapse Seismic Derived Information in a History Matching Procedure. *SPE EUROPEC/EAGE Annual Conference and Exhibition.* Vienna, Austria: SPE 143009.
STATOIL 2004. *Annual Reservoir Development Plan - Norne Field.*
STEPHEN, K. D., SOLDO, J., MACBETH, C. & CHRISTIE, M. 2006. Multiple-Model Seismic and Production History Matching: A Case Study. *SPE Journal,* SPE 94173, 418-430.
SZKLARZ, S. P. 2010. *History Matching via Ensemble Kalman Filter of Norne Field.* Master of Science, Delft University of Technology.
TOLSTUKHIN, E., LYNGNES, B. & SUDAN, H. H. 2012. Ekofisk 4D Seismic - Seismic History Matching Workflow. *SPE Europec/EAGE Annual Conference.* Copenhagen, Denmark: SPE.
USGS 2012. Body waves inside the earth. http://earthquake.usgs.gov: United States Geological Survey.
VERLO, S. B. & HETLAND, M. 2008. *Development of a field case with real production and 4D data from the Norne Field as a benchmark case for future reservoir simulation model testing.* Master's degree, NTNU.
WEISSTEIN, E. W. 2012. *Hessian* [Online]. From MathWorld--A Wolfram Web Resource. Available: http://mathworld.wolfram.com/Hessian.html [Accessed 3 Dec 2012].

Appendix A: SimOpt observed survey data file

```
'SEQNUM  '           1 'INTE'
          1
'INTEHEAD'          95 'INTE'
          0           0           2           0           0           0
          0           0          46         112          22      113344
          0           0           0           0           6           6
          0           7           3           0           0           0
         93           0           0           3           0           0
          0           0          19           0           0           0
         99           0           0           0           0           0
          0           0           0           0           0           0
          0           0           0           0           0           0
          0           0           0           0           0           0
          0           0           0           0           1           8
       2006           0           0           0           0           0
          0           0           0           0           0           0
          0           0           0           0           0           0
          0           0           0           0           0           0
          0           0           0           0          -1
'LOGIHEAD'          15 'LOGI'
 F  F  F  F  F  F  F  F  F  F  F  F  F  F  F
'DOUBHEAD'           1 'DOUB'
  0.173000000000000D+04
'STARTSOL'           0 'MESS'
'ACIP    '      113344 'REAL'
 -1.00000000e+33  -1.00000000e+33  -1.00000000e+33  -1.00000000e+33
 -1.00000000e+33  -1.00000000e+33  -1.00000000e+33  -1.00000000e+33
 -1.00000000e+33  -1.00000000e+33  -1.00000000e+33  -1.00000000e+33
  ... 113320 more values ...
 -1.00000000e+33  -1.00000000e+33  -1.00000000e+33  -1.00000000e+33
 -1.00000000e+33  -1.00000000e+33  -1.00000000e+33  -1.00000000e+33
 -1.00000000e+33  -1.00000000e+33  -1.00000000e+33  -1.00000000e+33
'eACIP   '      113344 'REAL'
  0.100000000e+02   0.100000000e+02   0.100000000e+02   0.100000000e+02
  0.100000000e+02   0.100000000e+02   0.100000000e+02   0.100000000e+02
  0.100000000e+02   0.100000000e+02   0.100000000e+02   0.100000000e+02
  ... 113320 more values ...
  0.100000000e+02   0.100000000e+02   0.100000000e+02   0.100000000e+02
  0.100000000e+02   0.100000000e+02   0.100000000e+02   0.100000000e+02
  0.100000000e+02   0.100000000e+02   0.100000000e+02   0.100000000e+02
'ENDSOL  '           0 'MESS'
```

Appendix B: Match Analysis of Case P – RMS and RMS Sensitivities

Name	Domain	RMS	Ztrans:Region1	Ztrans:Region2	Ztrans:Region3
Total	GLOBAL	562,46	4,3668	8,3685	-4,1163
WGOR	K-3H	18448	161,22	270,68	-159,58
WGOR	E-3AH	1175,9	0	0	0
WGOR	D-4AH	439,94	0	0	0
WGOR	B-1H	299,51	15,761	-12,256	12,768
WBHPH	E-3AH	274,54	0	0	0
WBHPH	E-4AH	259,84	0	0	0
WBHPH	B-1BH	247,63	1,7738	-1,3212	4,315
WBHPH	D-4AH	243,19	0	0	0
WBHPH	K-3H	242,94	2,1235	-1,8839	1,0684
WBHPH	D-3AH	228,76	0,87434	0,11385	1,547
WBHPH	B-4DH	228,18	4,0512	0,058129	1,8076
WGOR	D-2H	219,84	-31,816	35,781	-3,0906
WBHPH	D-1CH	217,87	-0,10171	-0,25562	1,12029
WBHPH	B-1H	213,82	4,5822	1,7986	1,3438
WBHPH	B-4H	205,1	0,43048	0,17805	1,2906
WBHPH	B-2H	202,4	0,9577	0,035858	0,78303
WBHPH	B-3H	201,95	3,0049	0,12611	1,3031
WBHPH	D-4H	197,41	0,48444	0,11649	1,8141
WBHPH	D-2H	196,79	4,0509	6,4098	0,64517
WBHPH	D-3BH	193,55	13,494	10,512	-6,6556
WBHPH	B-4BH	180,42	1,1084	12,84	2,9177
WGOR	E-4AH	176,88	0	0	0
WBHPH	E-3H	154,73	-0,29644	0,77018	-0,041544
WBHPH	E-2AH	154,02	-0,74138	18,926	-0,94507
WBHPH	D-1H	142,68	4,0741	-0,046921	0,17662
WGOR	B-4H	123,74	-1,186	-0,7908	2,7518
WBHPH	E-2H	122,45	-0,50527	47,922	0,245
WBHPH	E-1H	117,94	0,055652	49,018	0,73613
WGOR	B-4DH	99,488	19,343	5,3572	0,10705
WGOR	D-3AH	88,024	3,1501	2,6562	8,4066
WGOR	D-4H	87,502	-1,4669	-0,96703	-19,913
WGOR	D-1H	67,097	1,6161	0,31803	-0,0064929
WGOR	D-1CH	64,721	-11,534	-0,61776	-0,76315
WGOR	B-3H	62,024	2,0692	0,40357	9,9067

WBHPH	E-3CH	52,955	-0,30559	13,491	-0,72539
WGOR	E-2AH	52,758	-0,16538	-27,249	-0,19208
WGOR	D-3BH	48,261	21,57	0,58499	-25,105
WGOR	B-2H	31,158	-1,6398	-0,038603	0,11997
WGOR	B-1BH	29,011	6,7168	1,5059	5,0649
WGOR	B-4BH	28,188	-0,5664	-1,9388	-1,5275
WGOR	E-1H	23,015	-0,22246	-0,95639	-0,21706
WGOR	E-2H	21,871	-0,067375	-0,69113	0,35149
WGOR	E-3H	14,991	-0,072271	0,044468	0,0064104
WGOR	E-3CH	9,4429	-0,010573	1,0016	-0,001481
WWCT	E-3AH	2,3239	0	0	0
WWCT	D-1CH	2,1664	0,12388	-0,031268	-0,066369
WWCT	E-2AH	2,024	0,011563	0,066593	0,022476
WWCT	B-1BH	1,1726	-0,71421	0,082216	0,59074
WWCT	B-3H	0,77094	-0,078096	-0,005179	0,25882
WWCT	D-3AH	0,74907	0,14148	0,0026963	-0,26374
WWCT	E-3H	0,6843	-0,00044237	0,0012242	0,00037834
WWCT	D-1H	0,63037	-0,033133	0,00010859	-0,0029696
WWCT	D-3BH	0,62878	-0,17339	-0,15063	0,45899

Appendix C: Match Analysis of Case S – RMS and RMS Sensitivities

Name	Domain	RMS	Ztrans: Region1	Ztrans: Region2	Ztrans: Region3
Total	GLOBAL	4,93E+07	-4007,10	1884,70	368,20
dACIP-1.8.2001	1.8.2006-1.8.2001	4,93E+07	-4007,10	1884,70	368,20

Appendix D: Match Analysis of Case Auto – RMS and RMS Sensitivities

Name	Domain	RMS	Ztrans:Region1	Ztrans:Region2	Ztrans:Region3
Total	GLOBAL	4,9155E+07	50888	48726	-18965
Production	GLOBAL	4,7517E+07	6,0868E+05	6,9711E+05	-2,5417E+05
Survey	GLOBAL	4,9283E+07	7888,2	-1258,4	-832,91
WGOR	K-3H	1,5593E+09	3,1438E+07	2,337E+07	-9,1611E+06
WGOR	E-3AH	9,9137E+07	0	0	0
dACIP-1.8.2001	1.8.2006-1.8.2001	4,9283E+07	7888,2	-1258,4	-832,91
WGOR	D-4AH	3,7177E+07	0	0	0
WGOR	B-1H	2,7011E+07	1,4044E+07	-1,1947E+06	-8,8165E+05
WBHPH	E-3AH	2,317E+07	0	0	0
WBHPH	E-4AH	2,1931E+07	0	0	0
WBHPH	B-1BH	2,0883E+07	1,8431E+05	-1,08E+05	3,1523E+05
WBHPH	K-3H	2,055E+07	1,7352E+05	-1,6259E+05	66413
WBHPH	D-4AH	2,0523E+07	0	0	0
WBHPH	B-4DH	1,9352E+07	3,1412E+05	21673	1,1513E+05
WBHPH	D-3AH	1,9316E+07	2,1342E+05	11106	1,3254E+05
WBHPH	D-1CH	1,8402E+07	2,0565E+05	-20671	65570
WBHPH	B-1H	1,8187E+07	6,6423E+05	1,4483E+05	29963
WBHPH	B-4H	1,73E+07	61448	15391	82195
WBHPH	B-3H	1,7117E+07	4,4325E+05	15783	89431
WBHPH	B-2H	1,7099E+07	96017	3419	44152
WBHPH	D-3BH	1,6814E+07	1,0617E+06	8,5622E+05	-4,9658E+05
WBHPH	D-2H	1,6682E+07	-3,904E+05	5,423E+05	32600
WBHPH	D-4H	1,6654E+07	1,1094E+05	9239,4	1,1393E+05
WBHPH	B-4BH	1,5233E+07	3,7063E+05	1,0959E+06	1,6745E+05
WGOR	D-2H	1,5095E+07	-4,1088E+07	1,7144E+06	-1,726E+05
WGOR	E-4AH	1,4927E+07	0	0	0
WBHPH	E-3H	1,305E+07	-24749	64805	-3984,7
WBHPH	E-2AH	1,3023E+07	-42498	1,6158E+06	-84163
WBHPH	D-1H	1,217E+07	4,4474E+05	-1767,9	6159,5
WGOR	B-4H	1,0362E+07	-1,6155E+05	-51913	1,5016E+05
WBHPH	E-2H	1,033E+07	1,4538E+05	4,0448E+06	37852
WBHPH	E-1H	9,9654E+06	1,674E+05	4,1397E+06	36606
WGOR	B-4DH	8,3958E+06	-3,6744E+06	4,3848E+05	22524
WGOR	D-3AH	7,41E+06	1,1206E+06	2,1785E+05	1,4016E+06

WGOR	D-4H	7,3528E+06	-1,6946E+06	-70747	-1,1332E+06
WGOR	D-1H	5,741E+06	3,1116E+05	23035	-391,51
WGOR	D-1CH	5,2909E+06	1,2528E+05	-68947	-40317
WGOR	B-3H	5,2234E+06	6,3208E+05	60218	2,2841E+05
WGOR	D-3BH	5,1387E+06	2,0274E+06	1,6471E+05	-2,3701E+06
WGOR	E-2AH	4,5454E+06	50374	-1,8982E+06	-25151
WBHPH	E-3CH	4,4717E+06	-17271	1,1424E+06	-53723
WGOR	B-2H	2,5905E+06	-1,3462E+05	-2711,3	7396,4
WGOR	B-1BH	2,59E+06	1,113E+06	1,8112E+05	3,1439E+05
WGOR	B-4BH	2,3851E+06	14450	-1,6608E+05	-27756
WGOR	E-1H	1,941E+06	-8854,8	-81234	-5980,3
WGOR	E-2H	1,8365E+06	1541,9	-58727	29032
WGOR	E-3H	1,2625E+06	-6012,3	4247,7	660,46
WGOR	E-3CH	7,976E+05	-3598,6	64370	-415,46
WWCT	E-3AH	1,9616E+05	0	0	0
WWCT	D-1CH	1,8568E+05	752,42	-2742	-3054,2
WWCT	E-2AH	1,7139E+05	1742,1	5780	1114
WWCT	D-3AH	71598	15717	639,44	-11303
WWCT	B-1BH	67940	-72445	7075,2	38875
WWCT	B-3H	61674	933,04	-92,583	142,26
WWCT	B-1H	60034	-14302	29503	-941
WWCT	D-1H	52684	4164,1	-53,162	-116
WWCT	E-4AH	52551	0	0	0
WWCT	B-4DH	47873	4301,8	17832	5215
WWCT	B-2H	47746	4348	9189,7	4416
WWCT	E-3H	43846	-28,583	-22772	29
WWCT	E-1H	43169	-2909,1	16874	-3075
WWCT	E-2H	42505	-1573,7	13710	-1880
WWCT	D-4AH	41819	0	0	0
WWCT	B-4BH	32142	1202,3	-3993,7	2135
WWCT	D-4H	31751	2053,8	615,25	26
WWCT	D-2H	24863	449,54	-18158	42
WWCT	D-3BH	24375	-7424,2	14920	16643
WWCT	K-3H	13148	-528,49	231,24	33
WWCT	B-4H	177	-0,3254	1,9694	0